NTNU
Norwegian University of
Science and Technology

Time domain versus frequency domain VIV modelling with respect to fatigue of a deep water riser

Siren Therese Stien
Thorsen

Marine Technology
Submission date: June 2017
Supervisor: Svein Sævik, IMT

Norwegian University of Science and Technology
Department of Marine Technology

Preface

This report is the result of my master thesis for 5th year students at the Norwegian University of Science and Technology at department for Marine Technology, spring 2017. The topic is vortex induced vibrations on slender marine structures with focus on the difference between modelling in time domain and frequency domain with respect to fatigue.

I would like to thank my supervisors Professor Svein Sævik and PhD. Mats J. Thorsen at the Department of Marine Technology, NTNU, for weekly guidance and recommendations, both concerning the literature study, the development of the models and discussions about the differences in the two methods. I would also like to thank the members of office A.2.015 for their support during the work period.

The reader of this report should be familiar with basic theory of dynamic analysis. To understand technical expressions throughout the text it would be a great advantage to have knowledge of marine structures and hydrodynamic.

Trondheim, June 2017

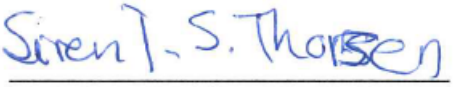

Siren Therese Stien Thorsen

Summary

In this thesis the new time domain model developed by PhD. Mats J. Thorsen is compared with the current practice, with respect to fatigue of a deep water riser. Current practice is to superposition the fatigue damage due to Vortex Induced Vibrations (VIV) obtained from the frequency domain and the first order wave dynamics from time domain analysis. Thorsen's model combines the Morison and VIV forces in one equation solved in the time domain. Thorsen's Model is implemented in RIFLEX which is compared with a superposition of RIFLEX for the time domain analysis and VIVANA for the frequency domain analysis for the current practice.

A riser installed at a water depth of 1200 meters with 2 meter elements is investigated. The cross section is constant for the whole riser with a diameter of 0.3 meters. The riser is subjected to sea stated based on data from the Norwegian Sea.

The fatigue analysis is carried out in MATLAB based on the result from RIFLEX, both for the new time domain model and for the dynamic analysis based on current practice. The stress standard deviation and maximum accumulated damage are found directly in VIVANA for the frequency domain model.

For the first cases investigated in this thesis, a mean current with no deviated waves, the two methods showed a good agreement for stress standard deviation and maximum accumulated damage. With applied waves, a good agreement for stress standard deviation were still obtained while the maximum accumulated damage showed some deviations. The maximum accumulated damage from the current practice was higher than for the new time domain method. This is due to the way fatigue is calculated, the accumulated damage is a function of the stress to the power of four. When the stress standard deviation is equal, one would expect equal damage as well. Since the current practice uses superposition is the total stress standard deviation from two different contributions while the new time domain method calculates it as one. The two contributions from the current practice raised to the fourth power and then added yields a smaller value compared to the total stress raised to the fourth power.

The second case, a one year current with and without waves, showed huge differences between the new time domain model and current practice. One reason for these huge differences might be that VIVANA uses frequency domain and the option simultaneously acting frequencies to calculate the response. The excitation zones where the dominating frequencies are acting, according to VIVANA, are at the bottom of the

riser while the new time domain model showed highest response at the upper half of the riser.

For the third case was response amplitude operators (RAOs) added to the model. The new time domain model was more affected by the RAOs than the current practice, but no huge differences in the fatigue damage because of the added RAOs.

The most important difference between the methods is the way fatigue damage is calculated. The current practice underestimates the maximum accumulated damage by use of superposition. Based on this is the new time domain model calculating a more accurate fatigue damage than the current practice.

Sammendrag

I denne avhandlingen er to metoder for beregning av utmatting av et dypvannsstigerør undersøkt. Den ene metoden er en tidsplanmodell utviklet av PhD. Mats J. Thorsen. Den andre er dagen praksis som bruker superponeringsprinsippet ved å legge sammen utmattingen fra frekvensplananalyse grunnet virvelinduserte vibrasjoner (VIV) med første ordens bølgedynamikk fra tidsplananalyse. Thorsens tidsplanmodell kombinerer Morison og VIV-krefter i en ligning. Thorsens modell er implementert i RIFLEX, og er sammenlignet med superponering av RIFLEX for bølgedynamikk i tidsplan og VIVANA VIV effekter i frekvensplan.

Stigerøret som er undersøkt er installert på 1200 meters vanndyp og er delt inn i elementer med 2 meters lengde. Flatearealet er konstant over hele stigerøret, med en diameter på 0.3 meter. Stigerøret utsettes for sjøtilstander basert på typiske data fra Norskesjøen.

Utmattingsanalysen er utført i MATLAB for resultatene fra RIFLEX, for både Thorsens tidsplanmodell og for den dynamiske analysen basert på dagens praksis. Standardavvik for stress og den maksimale akkumulerte skaden er i VIVANA funnet direkte i programmet.

I den første caseundersøkelsen, når kun strøm er påført, samsvarer modellene godt med henstn på standardavviket for spenning og maksimal skade. Når bølger blir påført samsvarer fortsatt standardavvik i spenning godt for de to modellene, mens maksimum akkumulert skade fra RIFLEX er høyere enn for nåværende praksis for alle kombinasjoner av bølgehøyde og bølgeperiode. Dette kommer av måten utmatting regnes på, hvor den maksimale skaden er en funksjon av spenningen opphøyd i fjerde. Når standardavviket for spenning er likt er det forventet at skaden også skal være lik, noe som ikke er tilfellet. Forskjellen på metodene som er sammenlignet, er at nåværende praksis bruker superponering. Standardavviket for spenning er en sum at to bidrag. Disse to bidragene er brukt hver for seg til å regne ut utmattingen noe som vil gi en lavere verdi. Opphøye to tall i fjerde for så å legge de sammen vil gi en lavere verdi enn å summere bidragene før de opphøyes i fjerde.

For den andre casen, en ettårsstrøm med kombinasjoner av bølger, som er undersøkt er det store forskjeller mellom den nye tidsplan modellen og nåværende praksis. En grunn til dette kan være måten VIVANA beregner frekvenser og dedikerer dem til forskjellige soner langs stigerøret. Plasseringen av de dominerende frekvensene fra VIVANA er

nederste del av stigerøret, mens den nye tidsplanmodellen gir størst utslag på øvre halvdel av stigerøret.

For den tredje casen ble respons amplitude operatorer (RAO) lagt til i modellen. Den nye tidsplanmodellen ble mer påvirket av bevegelsene enn det den nåværende praksisen, men ingen store endringer med hensyn på utmattingen ble kagt merke til.

Den største forskjellen mellom de to metodene er måten utmattingen beregnes. Den nåværende praksisen underestimerer den maksimale akkumulerte skaden ved bruk av superposisjon. Basert på dette beregner den nye tidsplanmodellen en mer nøyaktig utmatting i forhold til dagens praksis.

Scope of Work

NTNU Trondheim
Norges teknisk-naturvitenskapelige universitet
Institutt for marin teknikk

THESIS WORK SPRING 2017

for

Stud. tech. Siren Therese Thorsen

Time domain versus frequency domain VIV modelling with respect to fatigue of a deep water riser

Vurdering av tidsplan versus frekvensplan modellering mhp. utmatning av et dypvannstigerør

Drilling risers are subjected to both wave and current loads. The fatigue damage will have contributions from both 1st order and 2nd order floater motions, Morison forces and Vortex Induced Vibration (VIV) effects. The former is normally treated by time domain analysis (e.g. SIMA/Riflex) whereas VIV is normally treated by separate frequency domain models (e.g. VIVANA). Then the total fatigue is taken as the sum of the fatigue damages found from the two analyses. Recently a new time domain model has been developed by PhD student Mats Thorsen that combines the Morison and VIV forces into one equation. Then both current and wave effects can be included in the same analysis. The thesis work is to continue from the basis of the project of 2016 and will have focus on investigating the performance of the new time domain model as compared to existing procedures for calculating fatigue which is by super-positioning the fatigue damage obtained from the frequency domain model Vivana to those obtained from 1 order wave dynamics.

The work is to be carried out as follows:

1. Literature study into both time-domain and frequency domain models for Vortex Induced Vibration problem as applied to risers, including relevant standards for riser analysis and theoretical basis for riser time domain computational tools like Simla& Sima/Riflex and the frequency domain tools Vivana. Also familiarization with the tools Simla and Vivana to be used during the numerical studies.

2. Establish basis for case studies in terms of load cases, current profiles, wave scatter diagram, vessel motions, hydrodynamic coefficients, cross-section details, water depths and tension envelopes etc.

3. Establish Vivana and time domain models that can be used for further studies.

4. For selected sea states with combined action of wave and current, investigate the simulation length needed for the time-domain VIV model to obtain a stable standard deviation.

5. Perform fatigue analysis for selected sea states using the time domain VIV model and the standard model which is: Vivana for the VIV part and Riflex for the time-domain part. Compare the results and perform detailed investigations to explain eventual differences

6. Conclusion and recommendations for further work.

The work scope may prove to be larger than initially anticipated. Subject to approval from the supervisors, topics may be deleted from the list above or reduced in extent.

In the thesis the candidate shall present his personal contribution to the resolution of problems within the scope of the thesis work

Theories and conclusions should be based on mathematical derivations and/or logic reasoning identifying the various steps in the deduction.

The candidate should utilise the existing possibilities for obtaining relevant literature.

Thesis format

The thesis should be organised in a rational manner to give a clear exposition of results, assessments, and conclusions. The text should be brief and to the point, with a clear language. Telegraphic language should be avoided.

The thesis shall contain the following elements: A text defining the scope, preface, list of contents, summary, main body of thesis, conclusions with recommendations for further work, list of symbols and acronyms, references and (optional) appendices. All figures, tables and equations shall be numerated.

The supervisors may require that the candidate, in an early stage of the work, presents a written plan for the completion of the work.

The original contribution of the candidate and material taken from other sources shall be clearly defined. Work from other sources shall be properly referenced using an acknowledged referencing system.

The report shall be submitted in two copies:

- Signed by the candidate
- The text defining the scope included
- In bound volume(s)
- Drawings and/or computer prints which cannot be bound should be organised in a separate folder.

Ownership

NTNU has according to the present rules the ownership of the thesis. Any use of the thesis has to be approved by NTNU (or external partner when this applies). The department has the right to use the thesis as if the work was carried out by a NTNU employee, if nothing else has been agreed in advance.

Thesis supervisors:

Prof. Svein Sævik, NTNU
PhD. Mats J. Thorsen, NTNU
Deadline: June 11, 2017

Trondheim, January, 2017

Svein Sævik

Candidate – date and signature:

Nomenclature

Abbreviations

CF	Cross-flow
CFD	Computational Fluid Dynamics
DNV GL	Det Norske Veritas Germanischer Lloyd
FEM	Finite Element Method
IL	In-line
ISO	International Organization for Standardization
RAO	Response amplitude operator
VIV	Vortex induced vibrations

Roman Letters

Unfortunately many of the same roman letters have been used for more than one purpose, the exact meaning og each letter is therefore explained in the text.

A	Amplitude
A	Cross sectional area
C	Interception of N-axis in SN curve
$\mathbf{C}$	Damping matrix
$\mathbf{C_A}$	Added mass matrix
$\mathbf{C_L}$	Added damping matrix
C_v	Empirical force coefficient
D	Cylinder diameter
D	Accumulated damage
D_{VIV}	Accumulated fatigue damage from VIV
DFF_{VIV}	Design fatigue factor for VIV

$\mathbf{f}$	Volume force vector
f_0	Eigenfrequency in still water
$\mathbf{F_v}$	Strouhal force component
f_v	Vortex shedding frequency
$\mathbf{H}$	Transfer function matrix
$\mathbf{K}$	Stiffness matrix
k	Spring stiffness
L	Length of cylinder
$\mathbf{M}$	Mass matrix
m	Mass of cylinder
m	Slope parameter in SN curve
m_{a0}	Added mass of cylinder in still water
M_y	Moment about y-axis
M_z	Moment about z-axis
N	Number of cycles to failure
n	Number of stress cycles
N_x	Axial force
$\mathbf{R}$	External load vector
$\mathbf{r}$	Displacement vector
$\mathbf{R^E}$	External force vector
$\mathbf{R^S}$	Structural reaction force vector
Re	Reynolds number
St	Strouhal number
T	Time
t	Surface traction
t	Time
T_{design}	Design life time
U	Free stream velocity
$\mathbf{u}$	Displacement
V_R	Reduced velocity
W_y	Share modulus about y-axis
W_z	Share modulus about z-axis
$\mathbf{x}$	Transverse displacement
x_a	Amplitude of forced oscillations

Greek Letters

β	Bias factor
γ	Fatigue safety factor
ϵ	Natural strain tensor
θ	Angle
ν	Kinematic viscosity
ρ	Material density
ρ_f	Fluid density
σ	Stress
ϕ_v	Phase angle
ω	Load frequency
ω_c	Circular frequency
ω_v	Strouhal frequency

Contents

List of Figures

List of Tables

Chapter 1

Introduction

1.1 Background

As the search after oil and gas pushes operations further out into deeper water, several challenges emerge. One of them is vortex induced vibrations(VIV) of offshore structures, such as marine risers, due to ocean currents. VIV is a phenomenon important to include in dynamic analysis of marine risers and pipelines because it causes fatigue damage. As water depth increases the design and operation of risers gets more complex and VIV presents one of the biggest uncertainties facing riser engineers.

The methods for predicting VIV today is normally treated by frequency models like VIVANA. The problem with this is that the fatigue damage has contributions from both Morison forces and VIV effects. Morison forces is treated by time domain analysis like RIFLEX and SIMLA. Recently a new time domain model has been developed by PhD. Mats J. Thorsen that combines the Morison and VIV forces into one equation.

Thorsen's model is a new mathematical model of the hydrodynamic forces acting on a vibrating circular cylinder in a fluid flow. The basis of the model is that the total hydrodynamic force can be described as a sum of inertia, damping and vortex shedding forces. The hydrodynamic force model is formulated in time domain and implemented in RIFLEX and SIMLA [5].

1.2 Objectives

The purpose of this thesis is to compare the new time domain model developed by PhD. Mats Thorsen with current practice with respect to fatigue of a drilling riser.

The objectives are as follows:

- Literature study into both time domain and frequency domain models for Vortex Induced Vibration problem as applied to risers, including relevant standards for riser analysis and theoretical basis for riser time domain computational tools like SIMLA, RIFLEX and the frequency domain tools VIVANA. Also familiarization with the tools RIFLEX and VIVANA to be used during the numerical studies.
- Establish basis for case studies in terms of load cases, current profiles, wave scatter diagram, vessel motions, hydrodynamic coefficients, cross-section details, water depths and tension envelopes etc.
- Establish VIVANA and time domain models that can be used for further studies.
- For selected sea states with combined action of wave and current, investigate the simulation length needed for the time-domain VIV model to obtain a stable standard deviation.
- Perform fatigue analysis for selected sea states using the time domain VIV model and the standard model which is: VIVANA for the VIV part and RIFLEX for the time-domain part. Compare the results and perform detailed investigations to explain eventual differences
- Conclusion and recommendations for further work.

1.3 Thesis structure

Chapter 2 is a literature study into the phenomenon VIV. It takes into account what VIV is and how it occurs. In addition to this is different methods for predicting of VIV presented.

Chapter 3 presents the theory about fatigue calculation. All formulas used for calculations of fatigue damage in case studies later in the thesis are presented in this chapter.

Chapter 4 introduces different standards regarding fatigue of a riser. Both standards from Det Norske Veritas Germanischer Lloyd (DNV GL) and International Organization for Standardization (ISO) are presented.

Chapter 5 gets more into details of the computational tools that are used in this thesis. The program structure as well as the analysis method is presented for both RIFLEX and VIVANA. In addition to this is the Principle of Virtual Displacement presented as a method of solving finite element model (FEM) analyses.

Chapter 6 presents the model used in case studies in a later chapter. The layout of the riser is presented as well as stiffness parameters and cross sectional data. In addition to the model is load cases used in further studies presented.

Chapter 7 presents the analyze procedure for each analyze.

Chapter 8 presents the results form all analysis. The comparison of the two methods are discussed, as well as the the methods that lies behind the calculations.

Chapter 9 summarizes the analyze and presents the conclusion. In addition to this is recommendations for further work presented.

Chapter 2

Vortex Induced Vibration

Vortex induced vibrations (VIV) are vibrations caused by forces from vortices that are shed from both sides of a cylinder. The motions are caused by time varying forces on the body, acting in both cross-flow (CF) and in-line (IL) direction[2]. In order to provide a basic understanding of VIV, the fluid shedding process have to be looked more into.

2.1 Reynolds number and Strouhal number

Both Reynolds number (Re) and Strouhal number (St) is linked to the vortex shedding process. The Reynolds number is based on free stream velocity U and cylinder diameter D, where ν is the kinematic viscosity of the fluid. The Reynolds number is given in Equation (2.1).

$$Re = \frac{UD}{\nu} \tag{2.1}$$

Reynolds number defines the vortex shedding process, which is illustrated in Figure 2.1. At very low Reynolds numbers, below Re=5, the fluid flow follows the cylinder contours. In the range $5 \leq \text{Re} \leq 45$, the flow separates from the back of the cylinder and a symmetric pair of vortices is formed in the near wake. As the Reynolds number is further increased, the wake becomes unstable and one of the vortices breaks away [1]. It is convenient to divide the Reynolds number into different flow regimes. The different regimes in Table 2.1 is proposed by O. M. Faltinsen [6].

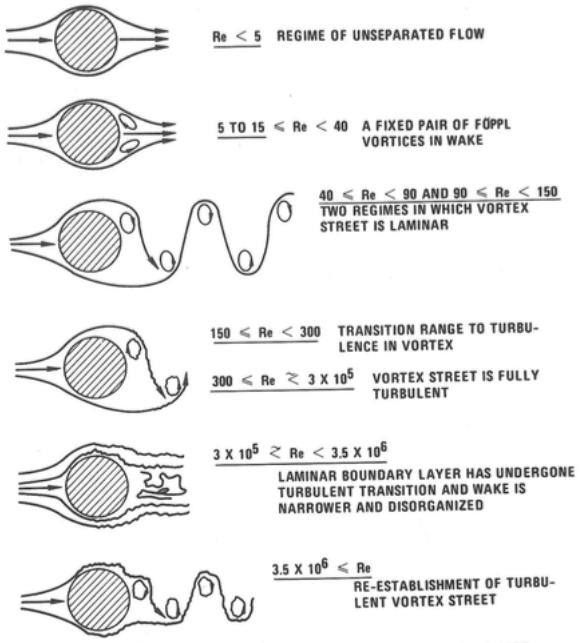

Figure 2.1: Regimes of fluid flow across a smooth circular cylinders [1].

Table 2.1: Flow regimes for different Reynolds number.

Flow regime	**Reynolds number**
Subcritical flow	$\mathrm{Re} \leq 2 \cdot 10^5$
Critical flow	$2 \cdot 10^5 \leq \mathrm{Re} \leq 5 \cdot 10^5$
Supercritical flow	$5 \cdot 10^5 \leq \mathrm{Re} \leq 3 \cdot 10^6$
Transcritical flow	$\mathrm{Re} \geq 3 \cdot 10^6$

Most VIV related experiments takes place in the subcritical regime, while full-scale cases easily will enter the critical and supercritical regimes. There is an uncertainty for empirical model since there are few data for experiments at high Re found in the open literature. It is, however, a common understanding that use of experimental data from the subcritical regime is conservative when applied on cases with higher Reynolds number [2].

The Strouhal number is a dimensionless proportionality constant between the predominant frequency of vortex shedding and the free stream velocity divided by the cylinder width. f_ν is the vortex shedding frequency, U is the free stream flow velocity approaching the cylinder, and D is the cylinder diameter [1]. The Strouhal number is given in Equation (2.2). It is found that the Strouhal number is a function of Reynolds number for a circular cylinder, this relationship is shown in Figure 2.2.

$$St = \frac{f_\nu D}{U} \tag{2.2}$$

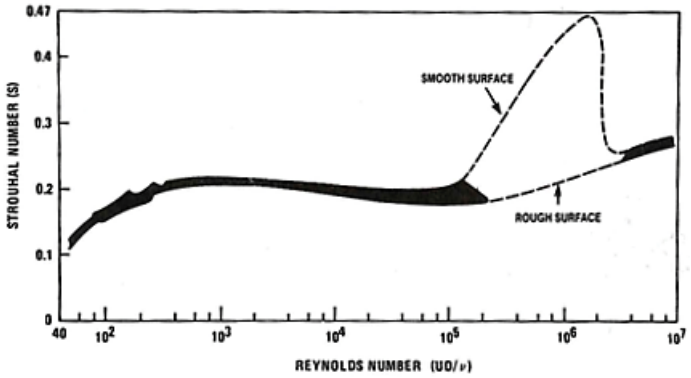

Figure 2.2: Strouhal number as a function of Reynolds number for a circular cylinder [1].

It can be seen from the figure above, Figure 2.2, that the Strouhal number is stable and close to 0.2 in the subcritical flow regime. In the critical and supercritical regime, the Strouhal number is strongly dependent on surface roughness. A rough surface will not see the dramatic increase from the subcritical regime to the critical regime, as a smooth cylinder will experience. In the transcritical regime, the Strouhal number becomes stable again and close to 0.26. In this regime, the roughness of the cylinder does no longer have an essential influence on the Strouhal number. Since the Strouhal number is a function of Reynolds number the shedding frequency can be found if the Reynolds number is given.

2.2 In-line and cross-flow forces

VIV can occur in two orthogonal directions. These two directions are cross-flow (CF), and in-line (IL) VIV. CF VIV is in the lift direction, transverse to the current, while IL VIV is in the drag direction, parallel to the current. Experiments show that the oscillations in lift force occur at the shedding frequency, while oscillations in the drag force occur at twice the shedding frequency [1]. The CF VIV is associated with larger reduced velocity values and larger oscillation amplitudes than the IL VIV [7]. When the vortex shedding frequency is close to an eigenfrequency for the structure CF VIV may occur. Knowing that the Strouhal number is close to 0.2 for actual Reynolds number, one may say that CF VIV may occur if

$$U \geq 5Df_0 \tag{2.3}$$

where U is the undisturbed flow velocity, D is the cylinder diameter and f_0 is the eigenfrequency in still water [2].

2.3 Added mass and response frequency

For structures in air, the vibrations occur at the structures eigenfrequency. For structures in water however, the picture is somewhat different as added mass plays a significant role in dictating the response frequency. The added mass is defined as the component of the hydrodynamic force which is in phase with the CF acceleration of the cylinder [2]. The still water eigenfrequency, f_0, of a cylinder is defined in Equation (2.4) below

$$f_0 = \frac{1}{3\pi}\sqrt{\frac{k}{m + m_{a0}}} \tag{2.4}$$

where k is the spring stiffness, m is the mass of the cylinder and m_{a0} is the added mass in still water.

For an oscillating cylinder the added mass will vary as a function of both the oscillating cylinder and response frequency, and not be a constant quantity. This means that for a given frequency and response amplitude, a specific added mass different from the still water added mass will be valid for the cylinder.

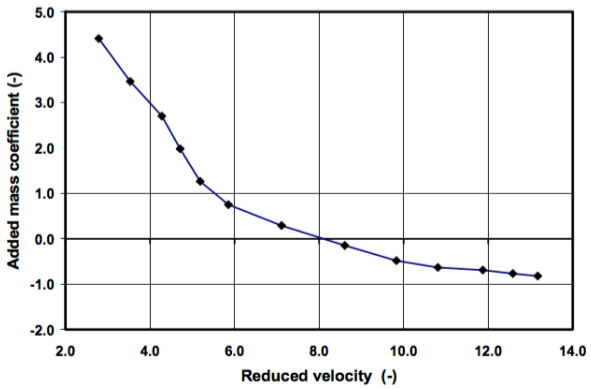

Figure 2.3: Added mass coefficient as a function of reduced velocity [2].

Figure 2.3 shows the added mass coefficient as function of reduced velocity found by Vikestad [8]. For the figure one can see that when reduced velocity is greater than eight the added mass is negative. Negative added mass is a consequence of the phase between the motion of the cylinder and the total hydrodynamic force. One way to find the added mass is to measure the force at one end of the cylinder. The force in phase with the acceleration may be found by Fourier decomposition. If the force from the physical mass of the cylinder is subtracted, the hydrodynamic mass of the cylinder is found. This is also known as the added mass. Another way to find the added mass is to assume that the oscillations occur at resonance. By using Equation (2.4) there is only one unknown, the added mass, since the cylinder mass and stiffness is known and the oscillation frequency is measured. Vikestad [8] found that the added mass from method one and two was equal.

2.4 Prediction of VIV

There are many different methods that are used to predict VIV. There exist both numerical, semi empirical and experimental methods. The experimental data help to verify the model predictions, thus leading to the most advantageous model framework [9]. There exist two different approaches for modelling the hydrodynamic forces acting on a slender marine structure, Computational fluid dynamics(CFD) and empirical methods.

2.4.1 Computational fluid dynamics

Computational fluid dynamics (CFD) is based on Navier-Stokes equations. These equations describe how the velocity, pressure, temperature, and density of a moving fluid are related [10]. By integrating the fluid pressure and the shear stresses around the surface, the forces acting on a structure can be found. CFD analysis is very time consuming and hence the use is limited.

There have been several attempts to apply CFD methods for simulation of VIV. However, many of these investigations are limited to 2D simulations at low Re number. Kinaci et al. [11] presented a study for Re$< 1.2 * 10^5$ where the 2D simulations by CFD overestimated the lift force. Rahman et al. [12] used CFD to study VIV effects for different aspect ratio (L/D) of a cylinder.

2.4.2 Semi-empirical methods

There exist several semi-empirical methods, in this section are different methods looked more into. The methods presented in this section are the MARINTEK model, SHEAR7, and ABAVIV. In addition to these models are VIVANA and RIFLEX presented in a later chapter.

MARINTEK model

Carl M. Larsen and Karl H. Halse presented a paper where they discussed commonly applied models to VIV [13]. One semi empirical model presented in this paper is the MARINTEK model, which is based on experiments by Sarpkaya [14]. This model does only consider CF VIV and does not take increased drag due to CF vibration into consideration. The transverse motion is found by direct time integration of the dynamic equilibrium by use of finite element model. The dynamic equilibrium is given as:

$$(\mathbf{M} + \mathbf{C_A})\ddot{\mathbf{x}}(\mathbf{t}) + (\mathbf{C} + \mathbf{C_L})\dot{\mathbf{x}}(\mathbf{t}) + \mathbf{K}\mathbf{x}(\mathbf{t}) = \mathbf{F_v}(\mathbf{t}) \tag{2.5}$$

M, **C** and **K** are respectively the structural mass, damping and stiffness matrices, which are constant during the time integration. x(t) represents the transverse displacements and the hydrodynamic loads are represented by $\mathbf{C_A}$, the added mass matrix, $\mathbf{C_L}$, the added damping matrix and $\mathbf{F_v}(\mathbf{t})$, the Strouhal load vector.

From Sarpkayas experiments are two coefficients, C_{mh} and C_{dh}, determined. C_{mh} is the force coefficient in phase with the cylinder acceleration while C_{dh} is the force coefficient in phase with the cylinder velocity. Based on these two coefficients are the MARINTEK coefficients, C_A and C_L defined as below:

$$\mathbf{C_A} = \mathbf{C_{mh}}\frac{\rho_f DLU^2}{2x_a\omega_c^2} \tag{2.6}$$

$$\mathbf{C_L} = \mathbf{C_{dh}}\frac{\rho_f DLU^2}{2x_a\omega_c} \tag{2.7}$$

where x_a is the amplitude of the forced oscillations, ω_c is the circular frequency of the forced harmonic motion, U is the fluid flow velocity, D is the diameter of the cylinder, ρ_f is the fluid density and L is the length of the cylinder.

The Strouhal force component, $\mathbf{F_v(t)}$ is found by

$$\mathbf{F_v(t)} = \frac{1}{2}\rho_f DLU^2 C_v sin(\omega_v t + \phi_v) \tag{2.8}$$

C_v is an empirical force coefficient, ω_v is the Strouhal frequency and ϕ_v is a phase angle between the force component and the motion of the cylinder. The C_v coefficient are in the MARINTEK model found from 2D experiments with fixed cylinders.

The time integration of the dynamic equilibrium in Equation (2.5) starts with the Strouhal force component $F_v(t)$ as the only excitation. As the response develops, the following four steps are carried [13]:

1. Based on the previous time history for the actual node is the amplitude and frequency of the response identified.
2. The reduced velocity of each node ia calculated as $V_r = \frac{2\pi U}{\omega_i D}$
3. By using the reduced velocity and amplitude as control parameters are the load coefficients C_L and C_A found by Equation (2.6) and (2.7).
4. The new coefficients are used to calculate the dynamic equilibrium in Equation (2.5), and the time integration is proceed.

A weakness with this method is that the model is based on a steady harmonic solution and therefore it questionable to application to problems involving time varying flow velocities. Another weakness is that the coefficients are based on experimental data using harmonic forced motion, which means one frequency, the model may then have problems with structures with many active frequencies. A positive side with the MARINTEK model is that the correlation length is not a problem since the response builds up the correlation itself.

SHEAR7

The first version of SHEAR7 was developed at Massachusetts Institute of Technology (MIT) in the early 1990s. SHEAR7 is a mode superposition program that uses frequency domain to calculate the VIV response. It can be used to predict the CF or pure IL VIV response of a long cylinder with varying tension in a sheared flow. The basic solution technique used is modal analysis and power balance iteration. The power balance iteration is used to account for the non-linear relationship between response and

lift coefficient. The power input and power output for each mode should be in balance in a steady state response. The program finds the lift and damping coefficients in a balanced state through iteration, starting with initial values for lift and damping. The converged lift and damping coefficients are used to compute the structure's response. An limitation for SHEAR7 is that it is not well suited to structures with large numbers of participating modes [15].

ABAVIV

ABAVIV is developed by Grant et al. [16] and is a time domain program to simulate the riser VIV using the finite element package ABAQUS along with VIV algorithm. This program is based on Blevins [1] correlation model. If the CF vibration is within a pre-defined lock-in criterion, the algorithm will tune the lift force to be in phase with riser vibration velocity. And if the CF vibration is not within the predefined lock-in area, the algorithm uses the Strouhal frequency as the lift force frequency and assign it a random phase angle for each correlation length along the riser [17].

Chapter 3

Fatigue

Marine structures are in general subjected to dynamic loads. Even if these loads are under yield stress at all time, microscopically changes in material will occur, which may develop into cracks over time. This is what we call fatigue and it is one of the main reasons that structures that are subjected to dynamic loads have a limited lifetime[18].

Fatigue damage estimation is performed based on long-term stress distribution and a material response model. For the material response model, either fracture mechanics or an SN curve approach can be applied[19]. In this thesis is the SN curve approach used.

3.1 Stress calculation

A structure subjected to loads will have different stress contribution along the surface depending on the direction of the load. For a circular cross section the stress along the surface are dependent on the local moments and the angel to the point. The stress can be calculated for different points around the cross section by use of Equation (3.1)[20].

$$\sigma = \frac{N_x}{A} + \frac{M_y}{W_y} cos\theta - \frac{M_z}{W_z} sin\theta \tag{3.1}$$

Here N_x is the axial force, A is the cross section area, M_y, W_y, M_z and W_z are respectively the moments and share modulus about y-axis and z-axis and θ is the angle to the point at the cross section. The definition of axis and direction are specified in Figure 3.1 below.

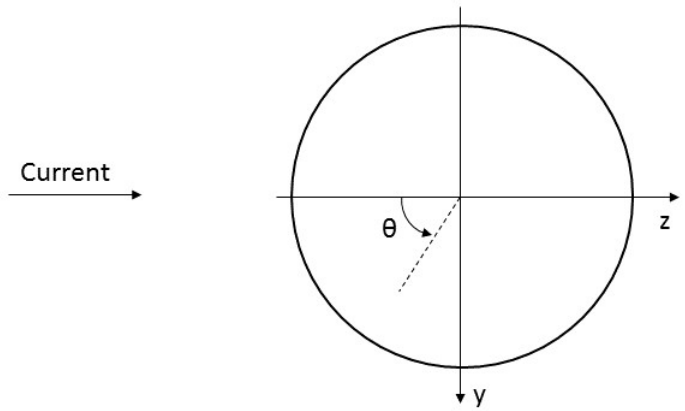

Figure 3.1: Circular cross section

3.2 SN curve

Most of the SN curve data are derived by fatigue testing of small specimens in test laboratories, where the specimens are subjected to stress ranges of varying amplitude until it reaches failure. The SN curve relate the stress range, $\Delta\sigma$, to the number of cycles before failure, N. For a straight-lined SN curve in log-log scale is the SN curve given as

$$N = C * \Delta\sigma^{-m} \tag{3.2}$$

where C is the interception of N-axis and m is the slope parameter.

Some materials responds different for low and high stress ranges and will therefore have a bi-linear SN curve. Such a curve is below in Figure 3.2.

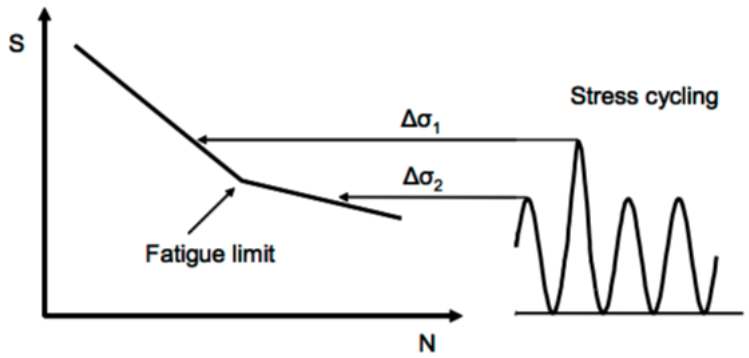

Figure 3.2: Bi-linear SN curve with an illustration of cyclic stress[3]

3.3 Cycle counting

To be able to calculate the damage from stress histories using SN curves, counting of stress cycles and stress levels must be performed. There exist many different counting methods some better than others. All good counting methods must count a cycle with the range from the highest peak to the lowest valley and must try to count other cycles in a manner that maximizes the ranges that are counted [21].

In this thesis will the most popular and probably the best method of cycle counting, according to Stephens and Fuchs[21] be used, the rainflow counting method. The operation of the rainflow method is shown in Figure 3.3. Here is the rainflow hysteresis loop down to the right while the stress response is left and strain response is upper right. The cycle starting with either the highest peak or lowest valley, in this case the lowest valley, point A on the figure. From here, go up to the next reversal, point B. The rainflow runs up and continues unless either the magnitude of the following valley is equal to or larger than the valley from which it initiated, or a previous rainflow encountered. Repeat the same procedure for the next reversal and continue these steps to the end. This procedure is repeated for all the ranges and parts of a range that were not used in previous steps. The rainflow counting results in a hysteresis loop with each closed loop representing a counted cycle.

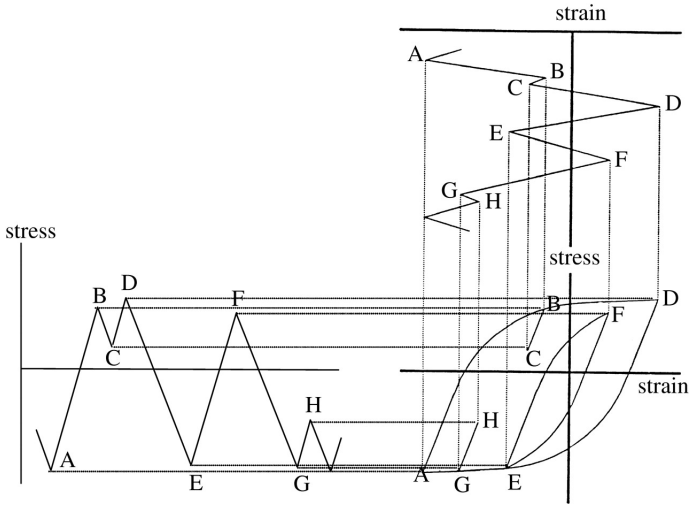

Figure 3.3: Rainflow counting [4].

3.4 Palmgren-Miner damage rule

The fatigue damage for long-term stress distribution can be found by using Palmgren-Miner damage rule. This rule states that the failure will occur when

$$\sum_{i=1}^{N_{\Delta\sigma}} \frac{n_i}{N_i} = 1 \tag{3.3}$$

where n_i is the number of stress cycles in the time history and N_{fi} is the number of cycles to failure for each stress cycle.

To calculate the fatigue damage per year is the total number of stress ranges per year, $n_{i,year}$, calculated by Equation (3.4), where T is the total time for the stress series.

$$n_{i,year} = \frac{n_i \cdot 365 \cdot 24 \cdot 60 \cdot 60}{T} \tag{3.4}$$

The accumulated damage is found by use of the number of stress ranges per year, $n_{i,year}$, and the corresponding cycles to failure, N_i, according to the SN curve. This is calculated from Equation (3.5).

$$D = \sum_{i=1}^{N_{\Delta\sigma}} \frac{n_{i,year}}{N_i} \tag{3.5}$$

Chapter 4

Standards

DNV GL describes them selves as an autonomous and independent foundation with the objectives of safeguarding life, property and the environment, at sea and onshore [22]. In addition to DNV GLs standards has the International Organization for Standardization (ISO)[23] a wide number of international standards. In this section are some of the guidelines developed by DNV GL and ISO regarding environmental loads, VIV and fatigue of risers considered.

4.1 DNV-RP-F204

The standard DNV-RP-F204 "Riser fatigue" [22] presents recommendations in relation to riser fatigue analyses based on fatigue tests and fracture mechanics. Chapter 4 in the standard handles VIV induced fatigue damage.

The acceptance criteria for VIV fatigue damage in DNV-RP-F204 presented as

$$\mathbf{D}_{VIV} \cdot \mathbf{DFF}_{VIV} \leq 1.0 \tag{4.1}$$

$\mathbf{D}_{VIV}$ is the accumulated fatigue damage from VIV over the life time of the riser, based on the long-term current distribution. In addition to the accumulated fatigue damage due to VIV, short-term extreme VIV events, such as VIV fatigue due to 100 year currents should be considered. $\mathbf{DFF}_{VIV}$ is the design fatigue factor for VIV. This value is dependent on the significance of the structural components with respect to structural integrity and availability for inspection and repair. For VIV this factor can

be calculated by a bias factor, β, and a VIV fatigue safety factor, γ. The VIV design factor is calculated for a specific design life time, $\mathbf{T}_{design}$, see Equation (4.2) below.

$$\mathbf{D}_{VIV}(\mathbf{T}_{design}) =\leq \frac{\beta}{\gamma} \tag{4.2}$$

4.2 DNV-RP-C205

Another standard, DNV-RP-C205 "environmental conditions and environmental loads" [24] gives guidelines for modelling, analysis and prediction of environmental conditions as well as guidance for calculating environmental loads acting on structures. Chapter 9 presents guidance on the calculation of environmental loads with respect to vortex induced oscillations as well as design criterion.

DNV-RP-C205 describes three different methods for prediction of VIV. Response based models is the first one. This is an empirical method providing the steady state VIV amplitude. The second method is force based models where the excitation, inertia and damping forces are obtained by integrated force coefficients established from empirical data. The last method is flow based models, which are based on CFD.

The zones where VIV may occur is in DNV-RP-C205 defined for both IL and CF VIV. The interval where VIV may occur is defined by the Strouhal number, St, and the reduced velocity, V_R. The IL vibrations may occur when

$$\frac{0.3}{St} < V_R < \frac{0.65}{St} \tag{4.3}$$

while CF vibrations may occur when

$$\frac{0.8}{St} < V_R < \frac{1.6}{St} \tag{4.4}$$

4.3 ISO 13623

Chapter 6 in ISO 13623 [23] handles rules and regulations of pipelines. In chapter 6.4.2.4 is the fatigue lifetime of a pipeline taken into account.

According to this chapter shall the fatigue analysis be performed on pipeline sections

and components that may be subject to fatigue from cyclic loads. This is done in order to demonstrate that initiation of cracking will not occur or define requirements for inspection for fatigue. Prediction of load cycles during construction and operation as well as translation of load cycles into stress and strain cycles shall be included in the fatigue analysis.

The fatigue resistance may be based on either SN data obtained on representative components or a fracture mechanics fatigue lifetime. When determining the fatigue resistance is it according to this chapter important to account for the effect of mean stresses, internal service, external environment, plastic pre-strain and rate of cyclic load. In addition to this is a safety factor included in the fatigue analysis. The selection of this factor shall take into account the inherent inaccuracy of fatigue-resistance predictions and access for inspection for fatigue damage. It may be necessary to monitor the parameters causing fatigue and to control possible fatigue damage accordingly.

Chapter 5

Computational Tools

In this thesis are two different computational programs used to investigate the VIV response of a drilling riser in deep water. The two programs are developed by SINTEF Ocean and named RIFLEX and VIVANA. Basic formulations and assumptions of the software are discussed in the following sections.

The following sections are based on the theory and user's manuals from RIFLEX and VIVANA, *RIFLEX Theory Manual V4.2v0* [25], *RIFLEX User's Manual V4.2rev0* [26], *VIVANA - Theory manual, version 3.7* [27] and *VIVANA 4.8.2 User Guide* [28].

5.1 The Principle of Virtual Displacement

The Principle of Virtual Displacement or Principle of Virtual Work is one of several ways of solving finite element model (FEM) analyses. The first step is to assume a displacement pattern between two known displacements values at the elements nodes. The external and internal work is then defined, and set to be equal to create a total equilibrium. By excluding volume forces, the total equilibrium can be expressed as

$$\int_V (\rho\ddot{\mathbf{u}} - \mathbf{f}) \cdot \delta\mathbf{u} dV + \int_V \sigma : \delta\epsilon dV - \int_S \mathbf{t} \cdot \delta\mathbf{u} dS = 0 \tag{5.1}$$

where ρ is the material density, $\ddot{\mathbf{u}}$ is the acceleration field, $\mathbf{f}$ is the volume force vector, σ is the Cauchy stress tensor, ϵ is the natural strain tensor, $\mathbf{t}$ is the surface traction and $\mathbf{u}$ is the displacement vector.

Systems with large displacements have to be solved by an incremental form of the principle of virtual displacement. There are two formulations that are widely used, the Total Lagrangian and the Updated Lagrangian. The difference between them is the choice of reference configuration. In the total Lagrangian formulation are the variables referred back to the initial configuration (C_0), while in the Updated Lagrangian are the variables referred back to the current configuration (C_n).

In addition to these two formulations is it sometimes convenient to relate the motion of material particles within a body to a local, rectangular coordinate frame, which translates and rotates along the average motion of the body. Co-rotated ghost reference is a formulation that takes this into account. The total motion is then found by combining the motion of the local position vector and the motion of the local reference system. In RIFLEX is the total Lagrangian used for bar elements and for beam elements is the co-rotated ghost frame used.

In order to use Equation (5.1) to develop finite element equations that can be implemented into a numerical code the following is needed[29]:

- Kinematics description; a relation between the displacement, rotations and the strains at a material point.
- A material law connecting the strain with resulting stresses.
- Displacement interpolation, describing the displacement and rotation fields by a number of unknowns on matrix format.

5.2 RIFLEX

RIFLEX is a computer program for analysis of flexible risers and other slender structures. The program computes static and dynamic characteristics of the structure.

5.2.1 Program structure

The program structure in RIFLEX is as shown below in Figure 5.1.

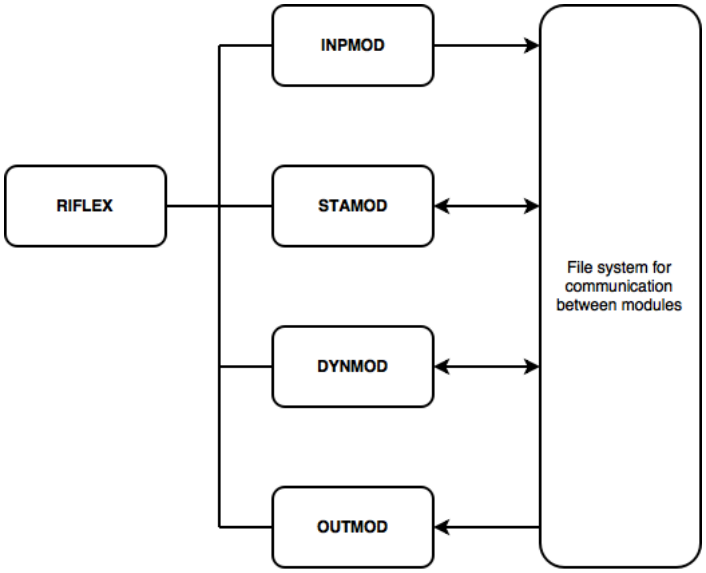

Figure 5.1: RIFLEX structure

The INPMOD file is the first one that has to be run. This file defines the model, its dimensions and material property. The environmental data is also presented in this file. After INPMOD has been run, several analysis can be performed by the other modules without rerun of INPMOD.

The static analysis is performed in STAMOD. STAMOD uses the input from INPMOD and defines the initial configuration for a succeeding dynamic analysis. The element mesh, stress free configuration and key data for finite element analysis are also generated in STAMOD.

The DYNMOD module carries out time domain dynamic analyses based on the final static configuration, environment data and data to define motions applied as forced displacements in the analysis. Before running DYNMOD, the IMPMOD and STAMOD modules have to be run.

Post processing of selected results generated by STAMOD and DYNMOD are done in OUTMOD. It is possible to store plots on a separate file as well as exporting time series via a standardized file format.

5.2.2 Analysis method

Static Analysis

The purpose of the static analysis is to determine the nodal displacement vector so that the complete system is in static equilibrium. This configuration is found by setting the internal structural reaction force, $\mathbf{R}^S$, equal the external force vector,$\mathbf{R}^E$. The force imbalance vector at incremental load step k is introduced as

$$\mathbf{R}_k(r) = \mathbf{R}_k^S(r) - \mathbf{R}_k^E(r) \tag{5.2}$$

where r is the nodal displacement vector including all degrees of freedom for the system. The static equilibrium is found by application of a incremental load procedure with equilibrium iterations at each load step. This is done by the Newton-Raphson iteration procedure in RIFLEX.

The Newton-Raphson method is the most frequently used iterative method for solving non-linear structural problems[30]. The algorithm to solve for r for the problem in Equation (5.2) equal to zero is given by:

$$r_{k+1} = r_k - \frac{\mathbf{R}(r_k)}{\mathbf{R}'(r_k)} \tag{5.3}$$

The iteration is stopped when the user defined accuracy is acceptable. The convergence criterion may be based on the change of displacement from one iteration to the next and expressed by

$$||\mathbf{r}_{k+1} - \mathbf{r}_k|| < \epsilon \tag{5.4}$$

where $||\cdot||$ is a vector norm and ϵ is a user defined error which normally is a small, positive number of magnitude $10^{-2} - 10^{-4}$.

Dynamic Analysis

The general equation of motion is given by

$$\mathbf{M}\ddot{\mathbf{r}} + \mathbf{C}\dot{\mathbf{r}} + \mathbf{K}\mathbf{r} = \mathbf{R} \tag{5.5}$$

where $\mathbf{M}$ is the mass matrix, $\mathbf{C}$ is the damping matrix, $\mathbf{K}$ is the stiffness matrix, $\mathbf{R}$ is the load vector and $\mathbf{r}$, $\dot{\mathbf{r}}$, $\ddot{\mathbf{r}}$ are respectively structural displacement, velocity and acceleration vectors.

The non-linear dynamic analysis is solved by direct time integration of the equation of motion. This can be done either with an explicit method, shown in Equation (5.6) or an implicit method, shown in Equation (5.7).

$$\mathbf{r_{k+1}} = \mathbf{f}(\ddot{\mathbf{r}}_\mathbf{k}, \dot{\mathbf{r}}_\mathbf{k}, \mathbf{r_k}, \mathbf{r_{k-1}}, ...) \tag{5.6}$$

$$\mathbf{r_{k+1}} = \mathbf{f}(\ddot{\mathbf{r}}_\mathbf{k+1}, \ddot{\mathbf{r}}_\mathbf{k}, \dot{\mathbf{r}}_\mathbf{k+1}, \dot{\mathbf{r}}_\mathbf{k}, \mathbf{r_k}, \mathbf{r_{k-1}}, ...) \tag{5.7}$$

Explicit methods are only dependent on information from the current and previous time step. These methods are conditionally stable and therefore very small time steps must be used. Implicit methods are dependent on information from the next time step in addition to information from the current time step. Since implicit methods use information at the next time step they will have better numerical stability than explicit methods. By use of information from the next time step an assumption on how the system accelerate between the time steps has to be done. Some basic examples are the constant average acceleration, linear acceleration and the constant initial acceleration[31].

5.3 VIVANA

VIVANA is a semi-empirical program for prediction of VIV for slender marine structures subjected to ocean current. The analysis method in VIVANA is based on FEM using beam or bar elements. The static condition is found from a general non-linear formulation that allows for very large displacements, but moderate strains. The dynamic analysis follows the frequency response method, which means that the VIV response must have small amplitudes relative to the length of the structure.

VIVANA will calculate the fatigue damage by assuming that the cross section is circular with a diameter defined from the cross section data. Stresses will also be calculated on the outer surface according to the cross section data. Three different analysis options are offered. These options are pure IL response, pure CF response and a combined

IL and CF analysis.

5.3.1 Program structure

As shown in the Figure 5.2 below is VIVANA linked to RIFLEX. RIFLEX runs bot INMPMOD and STAMOD modules before the VIVANA module can be run. The VIVANA module calculates the VIV response. These results are used to calculate fatigue damage and drag force amplification.

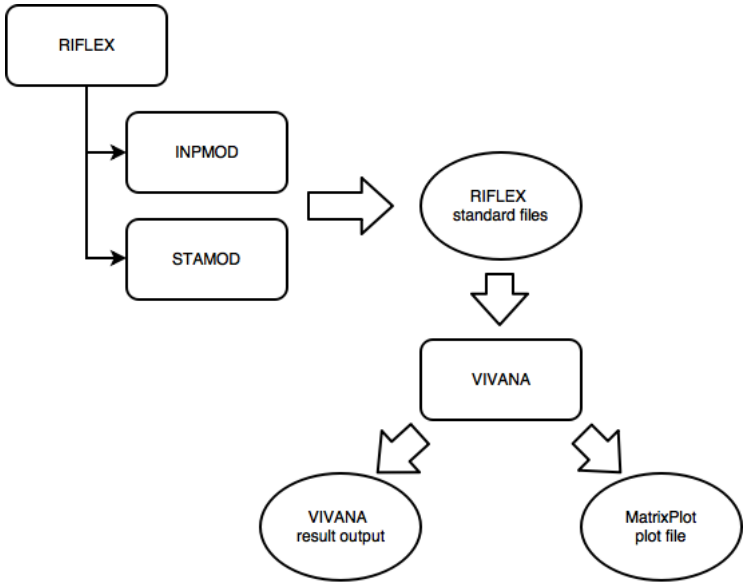

Figure 5.2: VIVANA structure

In this thesis has VIVANA been run trough a program called SIMA. SIMA is a tool developed by SINTEF Ocean for modelling and analysis of tasks within the field of marine technology.

5.3.2 Analysis method

The analysis method in VIVANA can be divided into the following nine steps.

1. Static analysis

In the first step is the static shape of the structure found. In addition to this is the normal flow velocity along the riser found based on the static shape and the current profile. This is done in RIFLEX and described in Section 5.2.2.

2. Eigenvalue analysis, still water

The eigenfrequencies and mode shapes of the structure in still water are found in step two. A sufficient number of eigenvalues will be found so that all possibly active VIV frequencies can be found when considering maximum vortex shedding frequency.

3. Identification of possible excitation frequencies

As the added mass for the riser will vary with VIV conditions, iteration is performed for the response frequency. Each of the eigenfrequencies found in step 2 are considered as a candidate for being exited by vortex shedding, iterations are carried out for each of the frequencies to find the complete set of possibly active eigenfrequencies.

4. Dedication of excitation zones

Each response frequency will be associated to an excitation zone where vortex shedding may excite the structure at the actual frequency. The zone is defined by an interval for the local non-dimensional frequency. The interpretation and use of the excitation zones can be done in two ways in VIVANA, either by simultaneously acting frequencies or by use of time sharing.

By use of simultaneously acting frequencies are all the frequencies acting at the same time. The dominating frequency is taking the total excitation zone, while other frequencies will take their zones from segments along the structure that have not been taken by frequencies with higher priority. When time sharing is used is each response frequency dedicated a time step when it is acting. The excitation zones are allowed to overlap, but they are not simultaneously active.

5. Calculation of CF response

The CF response is calculated by the frequency response method. The equation of motion is given in Equation (5.5), where the load vector may be written as a function of a complex vector $\mathbf{X}$ and the load frequency ω as shown in Equation (5.8).

$$\mathbf{R} = \mathbf{X}e^{i\omega t} \tag{5.8}$$

Similarly, the response vector, $\mathbf{r}$, is written as

$$\mathbf{r} = \mathbf{x}e^{i\omega t} \tag{5.9}$$

where $\mathbf{x}$ is a complex vector and ω is the response frequency.

By introducing the hydrodynamic mass and damping matrices dynamic equilibrium from Equation (5.5) can be expressed as

$$-\omega^2(\mathbf{M_S}+\mathbf{M_H})\mathbf{x}+i\omega(\mathbf{C_S}+\mathbf{C_H})\mathbf{x}+\mathbf{K}\mathbf{x}=\mathbf{X_L} \tag{5.10}$$

where $\mathbf{M_S}$ is the structural mass matrix, $\mathbf{M_H}$ is the hydrodynamic mass matrix and $\mathbf{C_S}$ is the structural damping. $\mathbf{C_H}$ is the hydrodynamic damping matrix and $\mathbf{X_L}$ is the excitation force vector. This equation can formally be expressed as

$$\mathbf{x}=\mathbf{H}(\omega)\mathbf{X_L} \tag{5.11}$$

where $\mathbf{H}(\omega)$ is the transfer function matrix.

6. Calculation of IL response

The IL response is calculated in the same way as CF response in step 5, but all data for hydrodynamic coefficients are different due to change from CF to IL response.

7. Calculation of fatigue damage

The fatigue is calculated on the basis of user defined SN-curves and the calculated response. The fatigue analysis can be performed in two different ways, either by time sharing or by simultaneously acting frequencies.

When time sharing is used is each of the possible response frequencies given a share of time where they will dominate. While for simultaneously acting frequencies are all the response vectors used in combination with the element stiffness matrices and cross section properties to arrive at time series of stress at the element ends. Stress cycles are counted by the rainflow counting method and fatigue damage is then found by Miner-Palmgren summation, these methods can be read more about in Chapter 3.

8. Calculation of drag magnification

A cross section that vibrates in CF direction will have larger drag coefficient than for the fixed cylinder case. To compensate for this is the drag magnification, $C_D(\frac{A}{D})$ calculated as in Equation (5.12) for each element i. The drag amplification factors, DAF, can be calculated in two different ways, either by Blevins formula, Equation (5.13), or by Vandiever, Equation (5.14).

$$C_D\left(\frac{A}{D}\right)_i = C_D(A=0)_i DAF\left(\frac{A}{D}\right)_i \tag{5.12}$$

$$DAF_{i,Blevins} = 1 + 2.1\left(\frac{A}{D}\right)_i \tag{5.13}$$

$$DAF_{i,Vandiver} = 1 + 1.043\left(\frac{2A_{rms}}{D}\right)_i^{0.65} \tag{5.14}$$

Where each element i have the diameter D, CF amplitude A, drag coefficient for fixed cylinder $C_d(A=0)$ and root mean square(rms) value of the response A_rms.

9. Storage of results for additional analysis by RIFLEX

The last stem is to store the results on VIVANA result files.

Chapter 6

Model and load cases

The model is built up by input files in both RIFLEX and VIVANA, which is attached in Appendix A. The environmental loads that are used are based on typical data from the Norwegian sea.

6.1 Model

In this thesis is a drilling riser at a water depth of 1200 meters studied. The riser is simplified to only consist of one pipe cross section, which means that the whole riser has the same diameter over the total length. The cross section that has been used is a axis symmetrical cross section represented by CRS1 in the INPMOD file which can be found in Appendix A.1. The dimensions of the cross sections and stiffness parameters are defined below in table 6.1. The stiffness parameters are also defined in the INPMOD file.

Table 6.1: Cross sectional data and stiffness parameters.

External cross sectional area	7.07E-02 m^2
Internal cross sectional area	6.16E-02 m^2
Mass per unit length	140 kg/m
Axial stiffness	1.91E+09 N
Bending stiffness	2.01E+07 Nm^2
Torsion stiffness	1.34E+07 $Nm^2/Radian$
Top tension	100E+03 N

The riser is modeled by two supernodes, one at the sea bottom and the other one at twelve meters above sea surface. Between the two nodes are the line segments, each of a length of two meters, which implies that it is 606 elements and 607 nodes including the two supernodes. The supernode on the sea bottom is fixed in all translations and rotation around z-axis to model that the riser goes into the sea bottom to drill the well. At the top is the supernode fixed in x- and y- translation as well as rotation around the z-axis. This is to model that the riser is fixed at a drilling platform. The riser modelled in VIVANA is shown in figure 6.1 where the grey surface represent the sea bottom, the blue surface is the water surface, the black vertical line is the riser and the green line is the applied current.

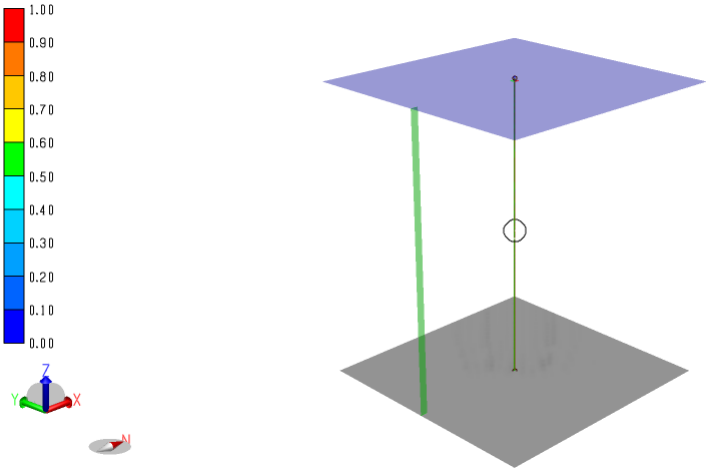

Figure 6.1: The riser modeled in VIVANA exposed to a current.

For calculation of the hydrodynamic forces are the nondenominational coefficients in Table 6.2 used. These coefficients are defined in the INPMOD file.

Table 6.2: Hydrodynamic force coefficients and capacity parameters

Quadratic drag coefficient in tangential direction	0
Quadratic drag coefficient in normal direction	1.3
Added mass per unit length in tangential direction	0
Added mass per unit length in normal direction	1
Linear drag force coefficient in tangential direction	0
Linear drag force coefficient in normal direction	0
Hydrodynamic diameter of pipe	0.3 m
Tension capacity	1E-06 kN
Maximum curvature	1 m^{-1}

In addition to the given coefficients above, some extra are defined in the RIFLEX model to calculate the VIV response. These coefficients will be looked more into in Section 8.1 where RIFLEX and VIVANA results are compared to give the same result. Below in Table 6.3 are the start values of the coefficients in RIFLEX listed.

Table 6.3: Coefficients in RIFLEX

Cv	1.3
FNUL	0.17
FMIN	0.125
FMAX	0.3
NMEM	500

6.2 Coefficients comparison

When the extra coefficients in RIFLEX are compared with VIVANA is the riser only subjected to current and no waves. This is done to only take the frequency analysis in VIVANA into account, and not the dynamic part in RIFLEX for the current practice. A very small wave is thus applied since RIFLEX needs wave parameters to be run. This wave is so small that is has no contribution to the analysis. The current that is applied is a typical mean current and is shown in Table 6.4.

Table 6.4: Current profile, mean current

Depth below sea surface $[m]$	current velocity $[m/s]$
20	0.22
50	0.21
100	0.19
200	0.18
300	0.17
400	0.17
500	0.14
600	0.13
800	0.13
1000	0.12
1197	0.12

6.3 Simulation length

When simulation length is investigated is the riser subjected to both current and waves. The current is the same as for comparison of coefficients, and is found in Table 6.4 while the wave data is found in Table 6.5. In this case is the current heading in the x-direction and the waves heading in negative y-directions, 90 degrees on the current.

Table 6.5: Wave parameters for investigating simulation length

Significant wave height, H_S $[m]$	2
Spectral peak period, T_P $[s]$	10

6.4 Fatigue analysis

For the fatigue analysis is an SN curve used to calculate the damage as described in Section 3.2. The SN data, interpolation of N-axis, C, and the slope, m, are given below in Table 6.6.

Table 6.6: Coefficients for SN curve

C	$10^{15.01}$
m	4

6.4.1 Case 1

For the first load case of the fatigue analysis is a mean current applied, as presented in Table 6.7. In addition to the current are four scenarios of a combination of wave height and wave period subjected to the riser. These scenarios are presented in Table 6.8. The waves are always applied in negative y-axis while the current is in positive x-axis, hence the waves are applied 90 degrees on the current.

Table 6.7: Current profile mean current

Depth below sea surface $[m]$	Current velocity $[m/s]$
20	0.22
50	0.21
100	0.19
200	0.18
300	0.17
400	0.17
500	0.14
600	0.13
800	0.13
1000	0.12
1197	0.12

Table 6.8: Combination of wave heights and wave periods for case 1

	Hs	Tp
Scenario 1	2	8
Scenario 2	2	10
Scenario 3	4	8
Scenario 4	4	10

6.4.2 Case 2

For case two in the fatigue analysis is a greater current applied. The current is a typical one year extreme current, which is presented in Table 6.9. As for case one in Section 6.4.1 is waves applied 90 degrees on the current in x-direction. The different combination of wave height and wave period is presented in Table 6.10.

Table 6.9: Current profile, one year extreme current

Depth below sea surface $[m]$	current velocity $[m/s]$
20	0.98
50	0.89
100	0.82
200	0.75
300	0.63
400	0.72
500	0.46
600	0.46
800	0.45
1000	0.44
1200	0.44

Table 6.10: Combination of wave heights and wave periods for case 2

	Hs	Tp
Scenario 1	2	8
Scenario 2	2	10
Scenario 3	4	8
Scenario 4	4	10

6.4.3 Case 3

In the third case is a response amplitude operators (RAO) for a deep water semisubmersible added to the model. An RAO file with transfer functions for each degree of freedom is supplemented to the INPMOD file. In addition to this is the plattform generated motions added to the dynamic analysis.

For this case is the same current as for case two in Table 6.9 used, as well as two combinations of wave height and wave period from Table 6.11.

Table 6.11: Combination of wave heights and wave periods for case 3

	Hs	Tp
Scenario 1	4	8
Scenario 2	4	10

Chapter 7

Analysis procedure

In this thesis are the two computation tools, RIFLEX and VIVANA, as described in Chapter 5 used to analyze the model in Section 6.1. The analysis is carried out in the following way described in this chapter using the load cases in Chapter 6.

7.1 Coefficients comparison

RIFLEX has some extra coefficients compared to VIVANA to calculate the VIV response, as mentioned in Section 6.1. To find the best values for these coefficients different values are tried out and compared with the current practice, which in this case is only VIVANA since no significant waves are acting. There are many different values that can be compared to decide the coefficients, in this thesis is the fatigue damage to be studied in later sections so the frequency is the most important parameter to compare.

FNUL is the first coefficient that is changed to get the frequency as similar as possible to the frequency in VIVANA. When the FNUL value is decided, is the Cv value changed to get the shape of standard deviation displacement as close as possible to the shape in VIVANA, without changing the frequency too much. The coefficients decided is a combination of the one giving the best fitted standard deviation and the closest frequency in VIVANA.

7.2 Simulation length

The response from environmental loads is developing over time. It is therefore important to make sure that steady state is obtained for the analyze time. The simulation length needed to obtain a stable result is investigated for the new time domain VIV model in RIFLEX

The investigation of the simulation length is done by starting with a short simulation length and increases it until steady state is reached. The criteria for obtaining steady state can be several like standard deviation displacement, standard deviation stress or frequency. In this case is the standard deviation displacement in CF direction used.

7.3 Fatigue analysis

The fatigue damage and stress standard deviation is calculated for different sea states presented in Section 6.4. The probability of the sea states are not taken into account, but modelled as the sea state is constant over the whole year.

In the current practice is the accumulated damage from VIV contribution calculated directly in VIVANA. The damage from VIVANA is added together with the accumulated damage calculated from the dynamic analysis in RIFLEX. The accumulated damage from the dynamic analysis is calculated in the same way as for the new time domain model in RIFLEX. These calculations are done in MATLAB and the scripts can be found in Appendix B. The same regards the stress standard deviation.

The calculations in MATLAB are based on the formulas in Chapter 3. The first script calls all the functions that is needed to determine the accumulated damage. The second one calculated the stress time series for each element based on the axial force and the moments. In the next script is the rainflow cycles counted. This is done by an extra package in MATLAB called WAFO. WAFO is a toolbox for statistical analysis and simulation of random waves and random loads and contain tools for fatigue analysis, sea modelling and statistics[32]. In the last script that is called, is the damage for each node calculated by an SN curve and Palmgren-Miner damage rule which is described in Section 3.2 and Section 3.4. This calculation of accumulated damage is done on 16 points around the cross section and the point with the maximum accumulated damage is then plotted. For the stress standard deviation is the MATLAB function std used to calculate the standard deviation of the stress time series.

The maximum accumulated damage as well as stress standard deviation for current practice and RIFLEX are plotted together and compared to each other.

Chapter 8

Presentation and evaluation of results

8.1 Coefficients comparison

Figure 8.1 shows the response standard deviation in CF direction, which in this case is in y-direction since the current is applied x-direction. The response standard deviation is plotted for VIVANA in black and different values of Cv and FNUL in RIFLEX for the remaining colours. Which color represent which values of Cv and FNUL can be found in the legend of the figure in addition to Table 8.1. In this table is also the frequency for each combination of coefficients presented.

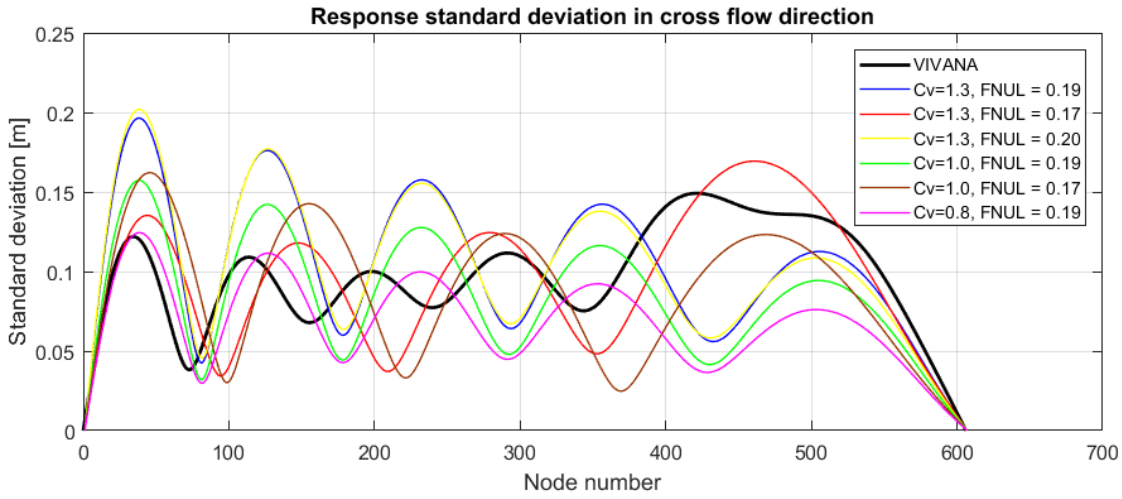

Figure 8.1: Response standard deviation, CF, for different Cv and FNUL values.

Table 8.1: Parameters for coefficients comparison

Cv	FNUL	Frequency [Hz]	Colour in Figure 8.1
0.17	1.3	0.086	red
0.19	1.3	0.106	blue
0.20	1.3	0.107	yellow
0.19	1.0	0.103	green
0.17	1.0	0.085	brown
0.19	0.8	0.102	magenta

For the same current as RIFLEX, VIVANA gives two dominating response frequencies. The first frequency is dominating from the bottom of the riser and 750 meters up and has a frequency of 0.083Hz. The other one is dominating on the rest of the riser length and has a frequency of 0.112Hz.

By looking at the response standard deviation in CF from VIVANA, one can see that it is mode five. For FNUL values 0.17 and below the mode is lower than the mode in VIVANA. Hence, the final FNUL value is chosen to be higher, and a value that give the same mode. When taking into account the frequency it would be beneficial to have a frequency that is between the two frequencies in VIVANA. This is the case for all the representatives with FNUL equal 0.19. Based on this is the FNUL value chosen to be 0.19. By looking at Figure 8.1 and take into account the shape and integral, the Cv value can be decided. The blue graph, Cv equals 1.3, lies above VIVANA for almost every node, while the magenta coloured graph, Cv equals 0.8, lies under VIVANA for the majority of the riser length. The green graph, Cv equals 1.0, lies above for some of the nodes and beneath for others and are hence the best fit to VIVANA with respect to the integral. The values that are used further in this thesis are presented in Table 8.2.

Table 8.2: Updated coefficients in RIFLEX

Cv	1.0
FNUL	0.19
FMIN	0.125
FMAX	0.3
NMEM	500

8.2 Simulation length

The response standard deviation in CF direction for combined loading of current and waves is presented in Figure 8.2 for different simulation lengths. The standard deviation increases as the simulation length increases. From T=500s, the brown graph in Figure 8.2, the standard deviation stars to be stable and does not change much when time increases. This implies that the simulation length needs to be at least 500 seconds to obtain a stable standard deviation.

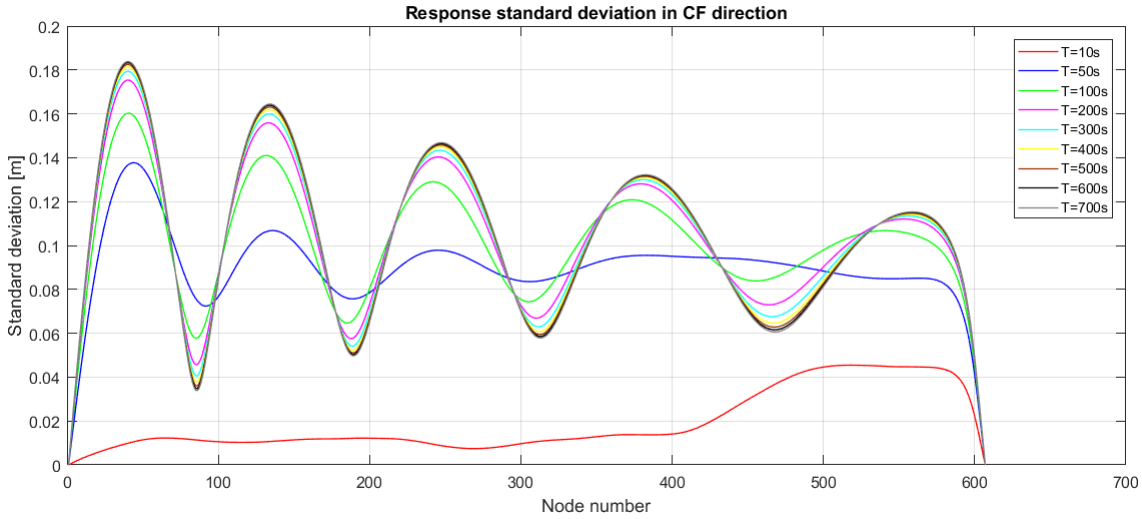

Figure 8.2: Response standard deviation, CF, for different simulation lengths.

8.3 Fatigue analysis

For the different load cases presented are both standard deviation stress and maximum accumulated damage plotted as a function of the riser length from bottom to top. The results from the current practice are always plotted in blue, while the results from RIFLEX are plotted in red. When the riser is subjected to both current and waves does the legend VIVANA in the figures represent the combination of the super-positioned result from VIVANA and RIFLEX.

For all the cases and scenarios is a figure of stress standard deviation presented as well as a figure with the maximum accumulated damage for the whole riser. For some of the figures are the differences in damage at top and bottom of the riser very big and a zoomed figure is thus presented for the bottom of the riser.

8.3.1 Case1

Figure 8.3 shows the stress standard deviation for a mean current without any significant waves. The current practice, which is only VIVANA, shows good agreement in both shape and magnitude compared to RIFLEX. The mode for both of the programs are the same, but with an offset compared to each other. When looking at the maximum accumulated damage in Figure 8.4, the same trends as for the stress standard deviation is seen. The damage is a function of the stress in the power of four, which implies that stress standard deviation and maximum accumulated damage will have the same shape as seen from the Figures 8.3 and 8.4. RIFLEX has higher amplitude for stress standard deviation as well as for maximum accumulated damage as expected.

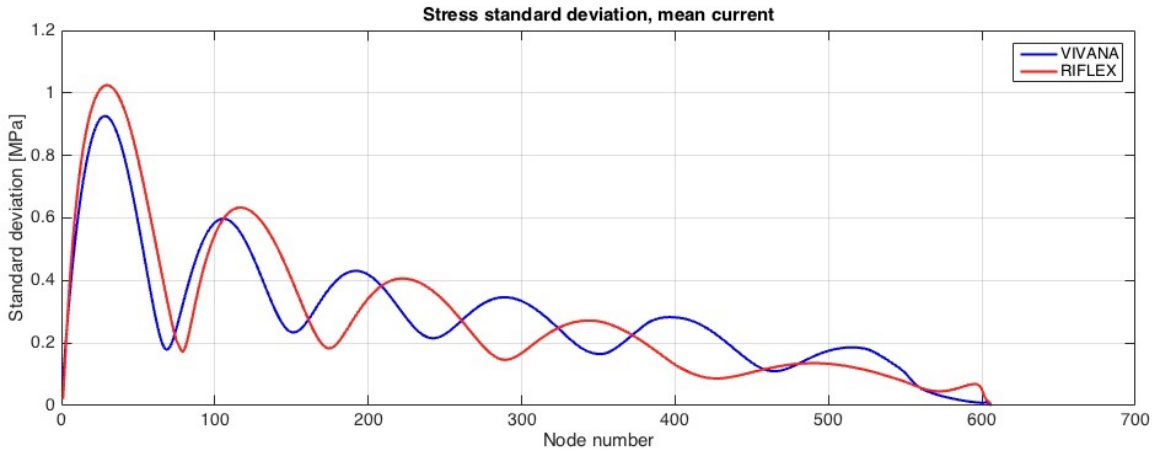

Figure 8.3: Stress standard deviation for a typical mean current.

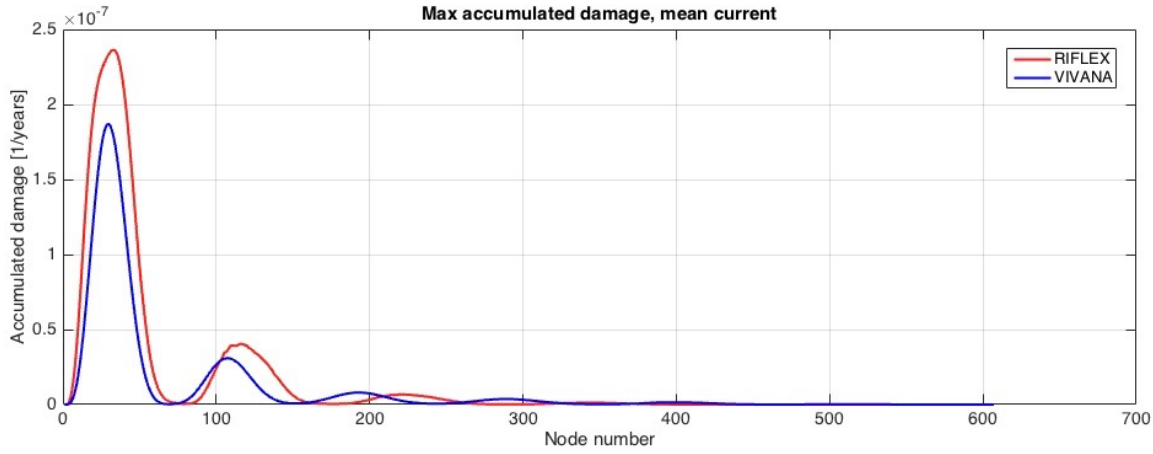

Figure 8.4: Maximum accumulated damage for a typical mean current.

Scenario 1

The stress standard deviation for the first scenario is presented in Figure 8.5. The standard deviation for current practice is a bit higher than the one for the new time domain model. The dynamic analyze has now given a contribution in the top of the riser which is seen from the figure as a very high peak in the stress standard deviation figure. The peak of the dynamic analyze appears in the maximum accumulated damage in Figure 8.6 as well as for the stress standard deviation. RIFLEX gives higher maximum accumulated damage for the majority of the riser compared to current practice. In the zoomed part of the Figure 8.6 is RIFLEX higher than current practice despite that the stress standard deviation from the current practice was higher than for RIFLEX.

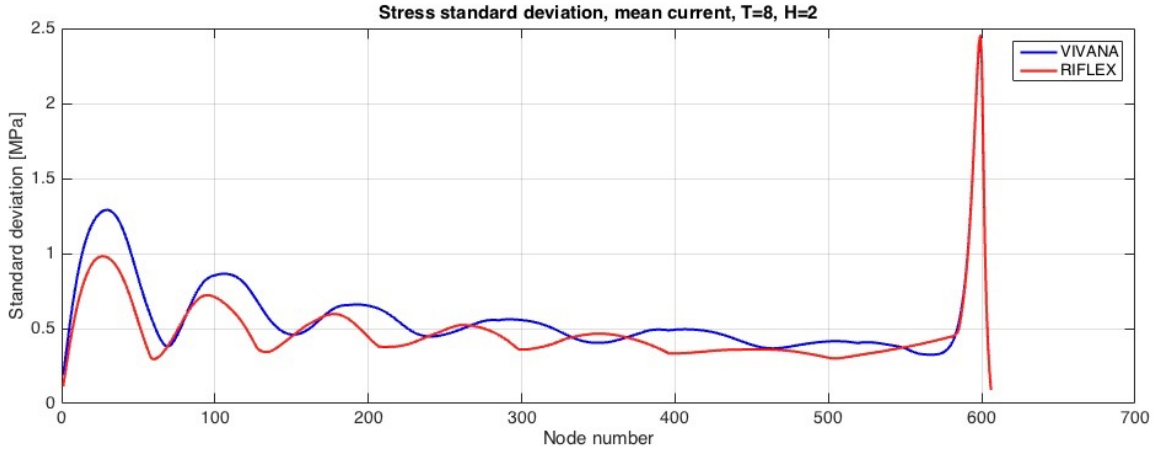

Figure 8.5: Stress standard deviation for a typical mean current and waves with Hs=2m ans T=8s.

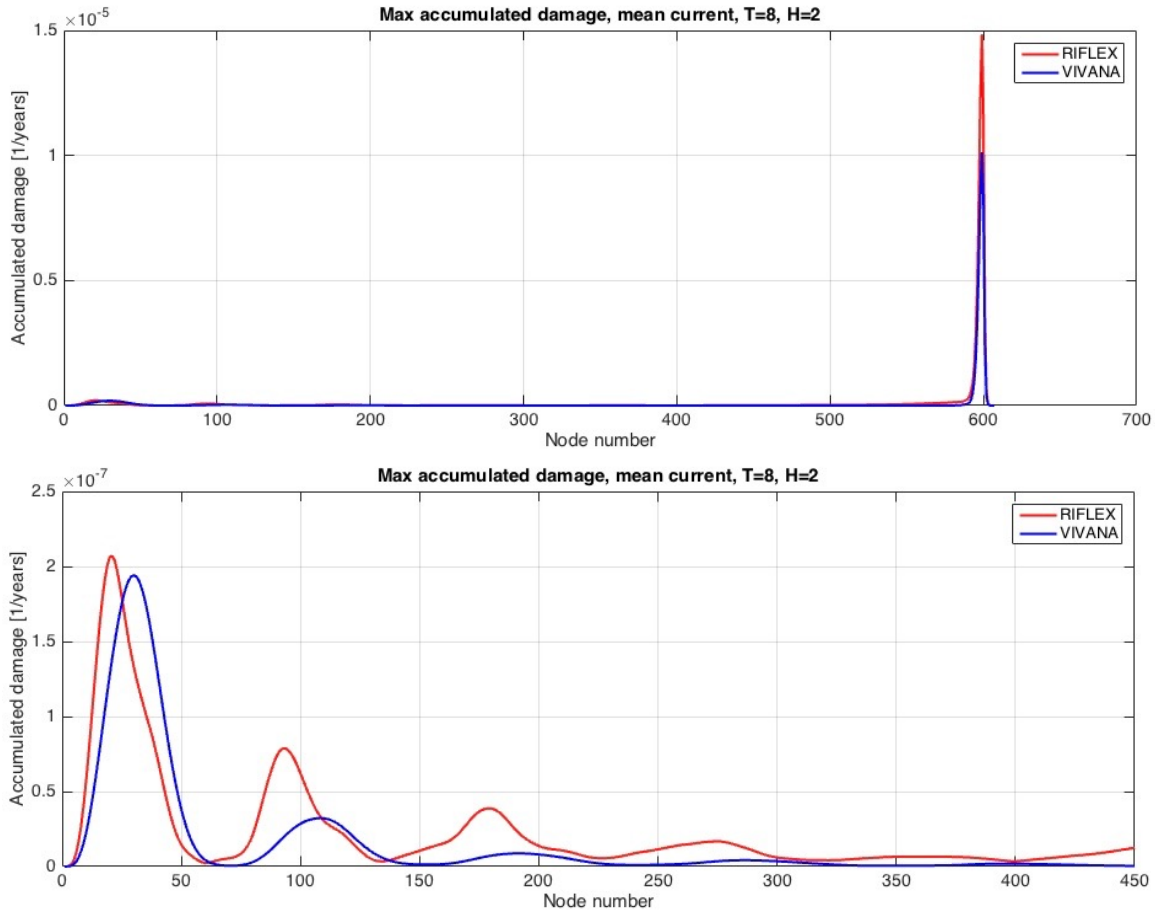

Figure 8.6: Maximum accumulated damage for a typical mean current and waves with Hs=2m and T=8s.

Scenario 2

Figure 8.7 and Figure 8.8 presents respectively the stress standard deviation and the maximum accumulated damage for scenario two. The stress standard deviation for the current practice lies slightly above stress standard deviation from RIFLEX through the whole riser. Regarding the accumulated damage is the values from RIFLEX higher than the values for current practice for both the top and bottom of the riser.

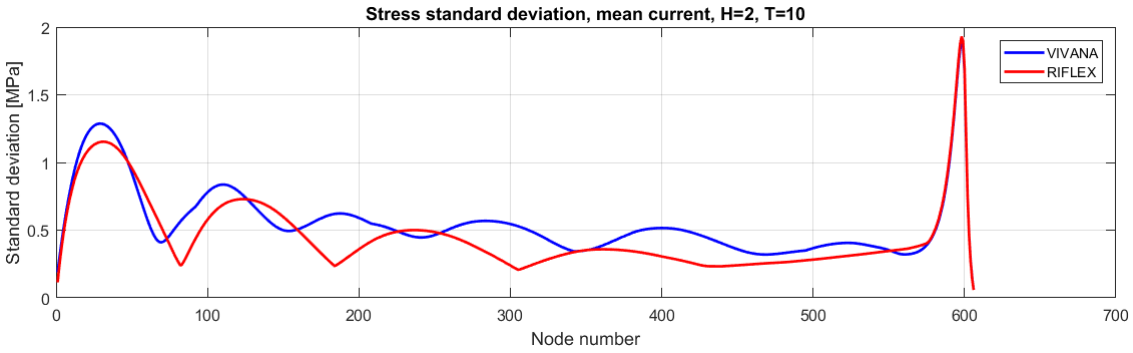

Figure 8.7: Stress standard deviation for a typical mean current and waves with Hs=2m ans T=10s.

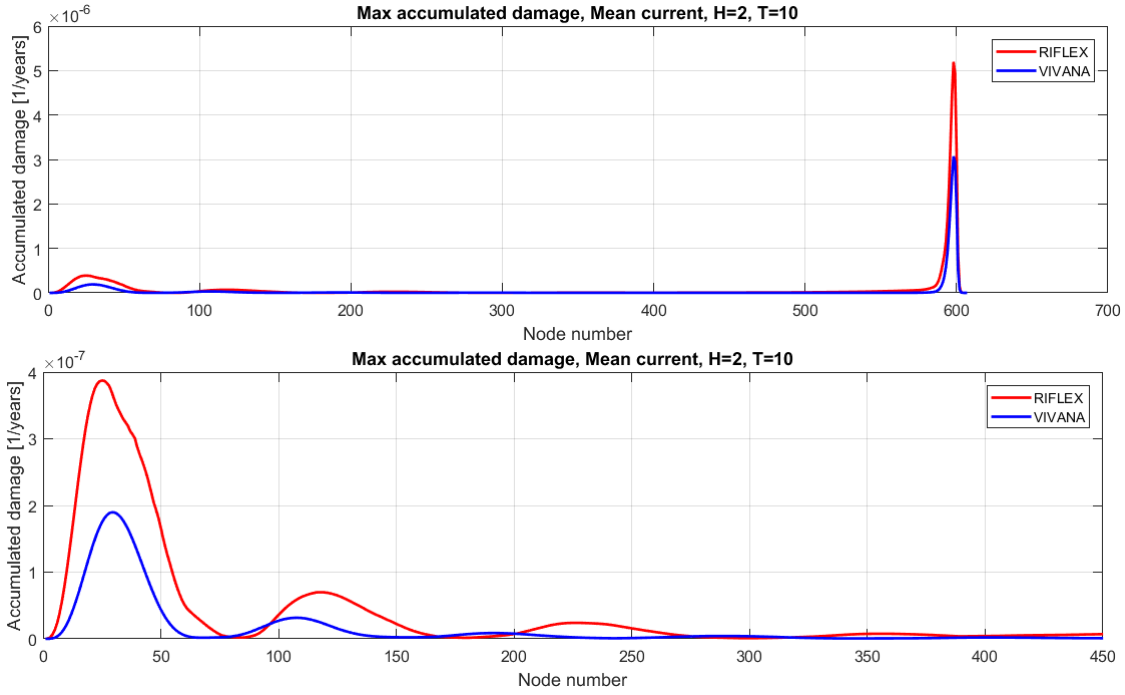

Figure 8.8: Maximum accumulated damage for a typical mean current and waves with Hs=2m and T=10s.

Scenario 3

In this scenario is the stress standard deviation presented in Figure 8.9 almost identical for current practice and RIFLEX. The maximum accumulated damage in Figure 8.10 for current practice and RIFLEX is deviating, despite the identical stress standard deviation. There are huge differences in the damage, especially at the bottom and top of the riser.

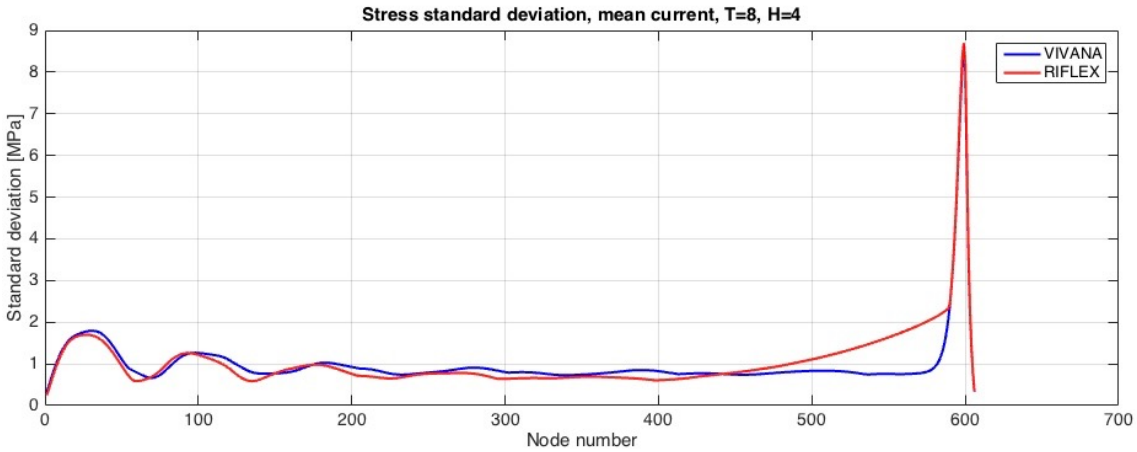

Figure 8.9: Stress standard deviation for a typical mean current and waves with Hs=4m ans T=8s.

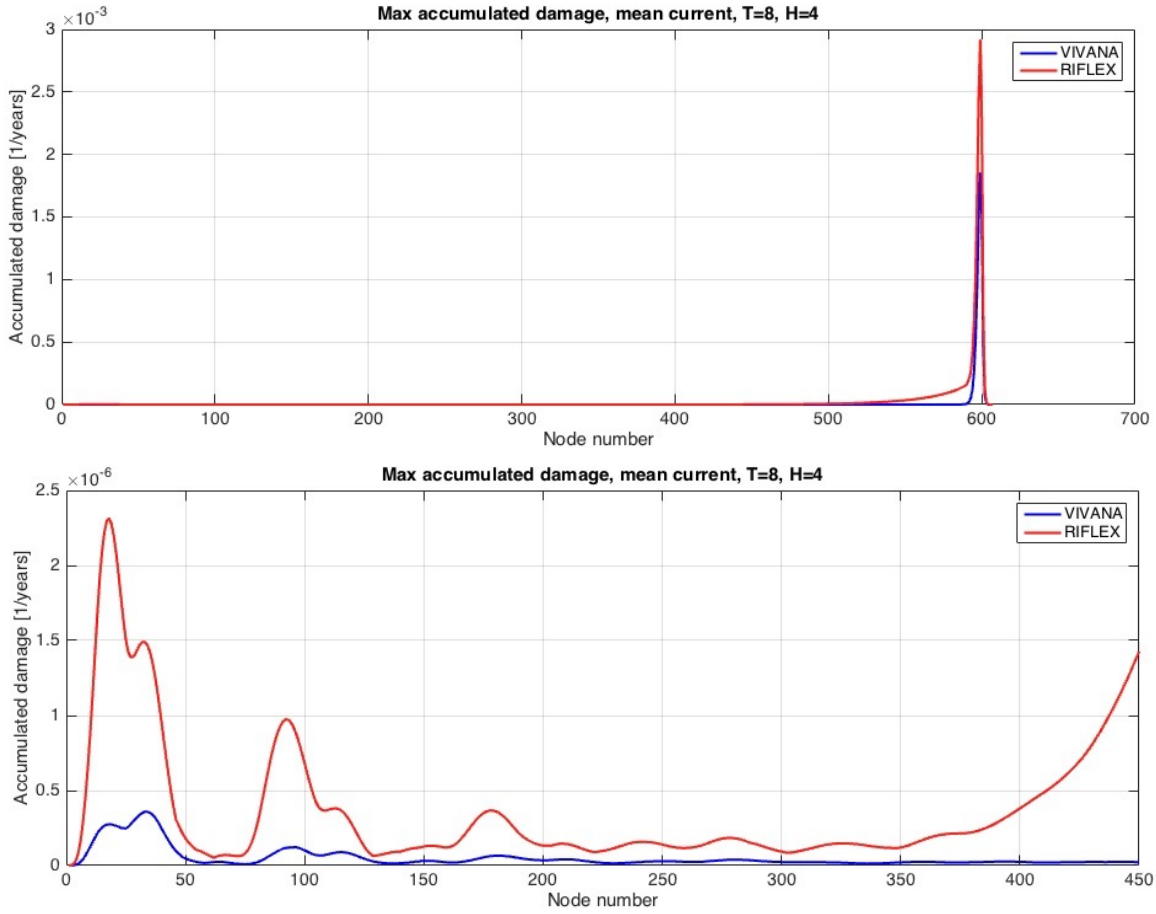

Figure 8.10: Maximum accumulated damage for a typical mean current and waves with Hs=4m and T=8s.

Scenario 4

Figure 8.11 shows that the stress standard deviation for current practice lies right above RIFLEX as for almost all of the other scenarios. The maximum accumulated damage is presented in Figure 8.12 and illustrates that the damage for RIFLEX lies above the damage for the current practice. This applies both for the top of the riser as well as for the bottom of the riser.

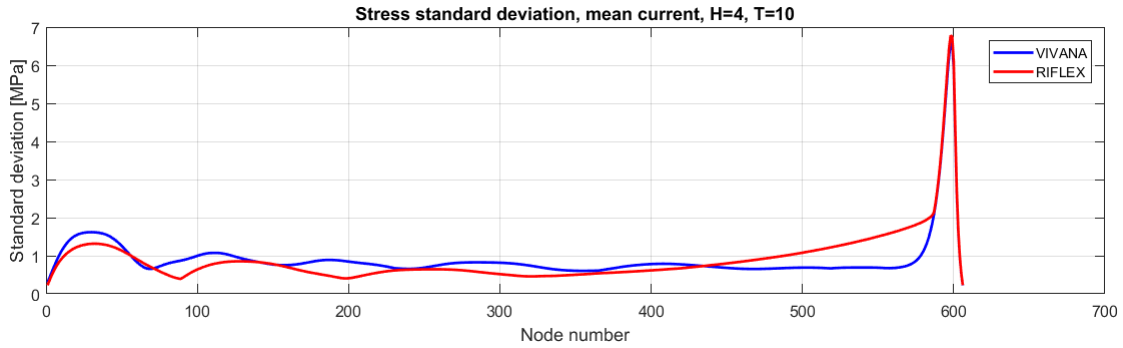

Figure 8.11: Stress standard deviation for a typical mean current and waves with Hs=4m ans T=10s.

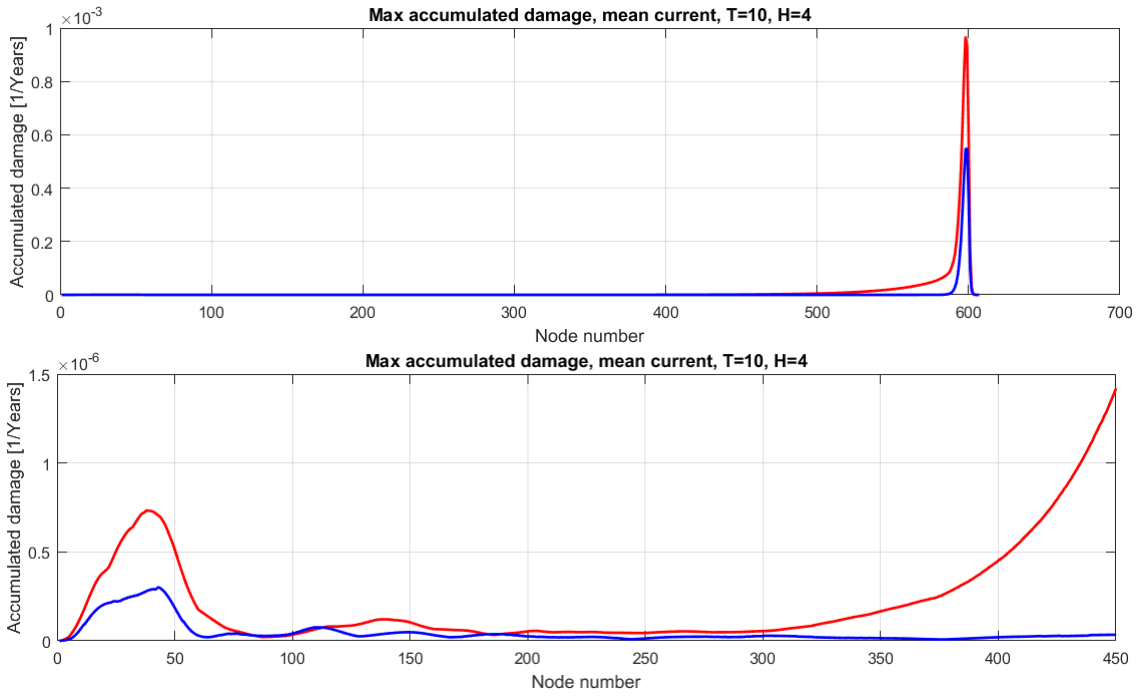

Figure 8.12: Maximum accumulated damage for a typical mean current and waves with Hs=4m and T=10s.

Evaluating of scenarios

The trend that recur for all the scenarios in case 1, that the stress standard deviation for the current practice is higher or equal compared to RIFLEX while the maximum accumulated damage is highest for RIFLEX for all scenarios, has with the way the fatigue is calculated. In RIFLEX is the stress standard deviation calculated form one time series while the stress standard deviation for the current practice is calculated by superposition. The stress standard deviation from VIVANA is calculated directly by use of the frequency domain and is added to the stress standard deviation calculated from the time series by the dynamic analysis from RIFLEX.

As mentioned earlier is the accumulated damage a function of the stress in the power of four. Because the current practice uses superposition will the accumulated damage be lower than the accumulated damage calculated from RIFLEX when the dynamic analysis have a contribution to the stress standard deviation. This is seen by Equation 8.1 below.

$$(\Delta\sigma_{new\ time\ domain\ model})^4 > (\Delta\sigma_{VIVANA})^4 + (\Delta\sigma_{RIFLEX})^4 \tag{8.1}$$

The accumulated damage is super-positioned and the stress standard deviation from VIVANA is right below one mega pascal while the stress standard deviation from the dynamic analysis that is added to VIVANA lies between a half and one mega pascal. When these two are calculated separately will the accumulated damage be a function times $1^4 + 1^4 = 2$. For the new time domain analysis in RIFLEX is the stress standard deviation right below two mega pascal and the accumulated damage will be a function times $2^4 = 16$. A factor of two and 16 is a huge difference and is the reason why the current practice and the new time domain model in RIFLEX gives different results for maximum accumulated damage, when the stress standard deviation is quite similar.

8.3.2 Case2

The stress standard deviation for the riser subjected to only current in case two is presented in Figure 8.13. The figure shows that it is huge differences from the current practice and RIFLEX. The current practice gives highest response in the bottom of the riser, from 600 meters below sea surface and down, while RIFLEX gives highest response on the top of the riser. One reason for this might be that VIVANA uses

frequency domain and the option simultaneously acting frequencies is used. For this option will each frequency be associated to an excitation zone and the frequencies excited in the top of the riser gives small displacement amplitudes compared to the once further down. The excitation zones for this case in VIVANA is shown in Figure 8.14. The excitation zone for the lower 750 meters of the riser have a response amplitude which is a factor of ten higher than all the other active frequencies.

In Figure 8.15 is the maximum accumulated damage presented. RIFLEX gives much greater damage than VIVANA for this case. This is related to the stress standard deviation and is expected after seen the figure for stress standard deviation.

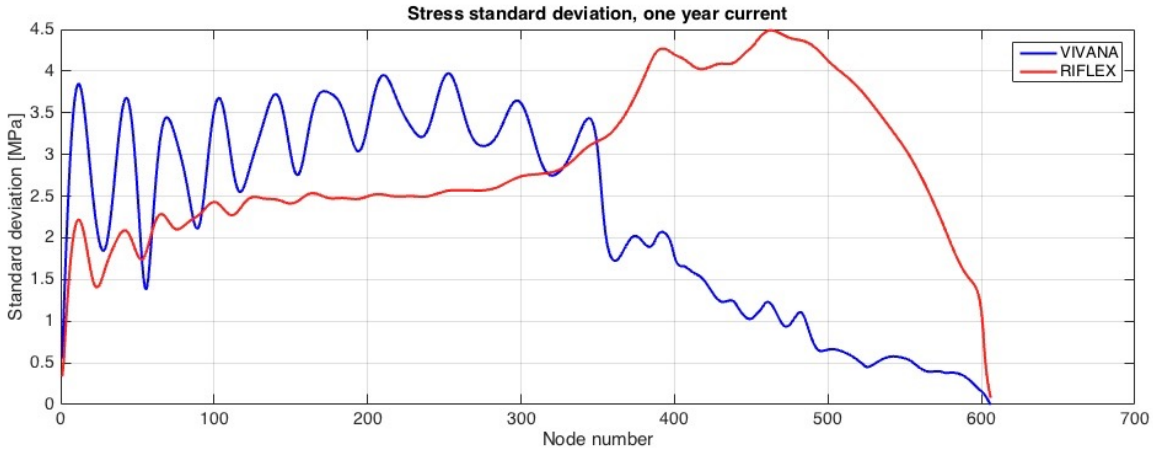

Figure 8.13: Stress standard deviation for a typical one year extreme current.

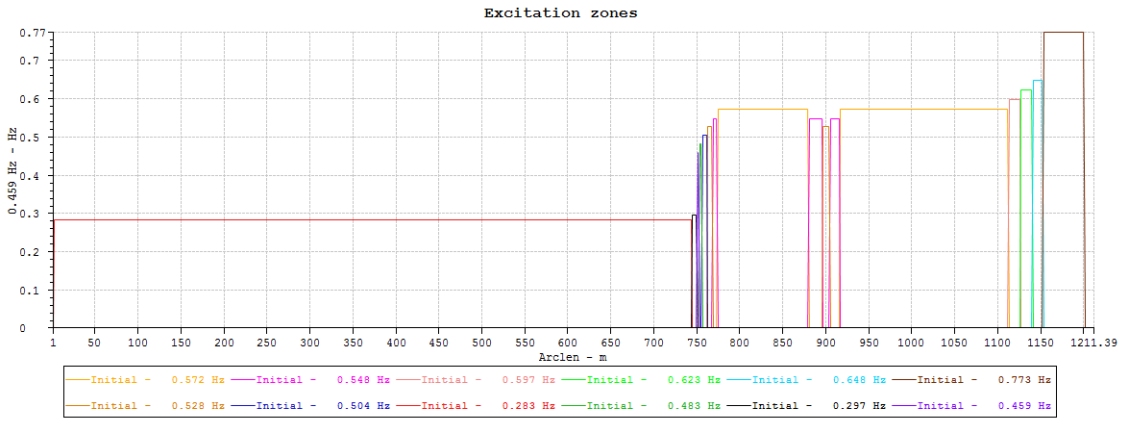

Figure 8.14: Excitation zones from VIVANA.

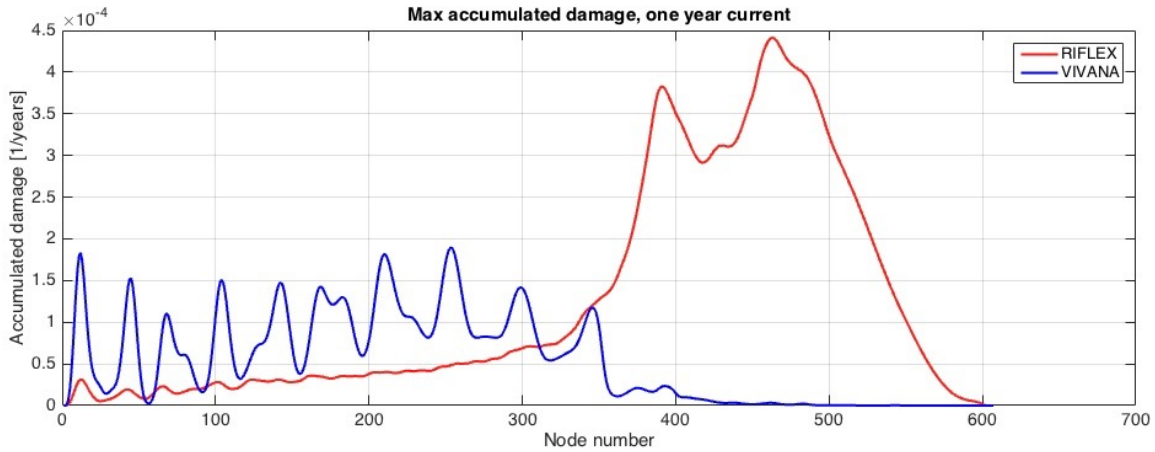

Figure 8.15: Maximum accumulated damage for a typical one year extreme current.

Scenario 1

As for the case with only current is the stress standard deviation in Figure 8.16 for the current practice and RIFLEX pretty different. Compared to the case without waves has the peak from the current practice in the upper half of the riser decreased, and for the lower half has the stress standard deviation increased. At the top of the riser has the contribution from the waves increased the stress standard deviation for both current practice and RIFLEX. The maximum accumulated damage presented in Figure 8.16 have the same shape as the stress standard deviation.

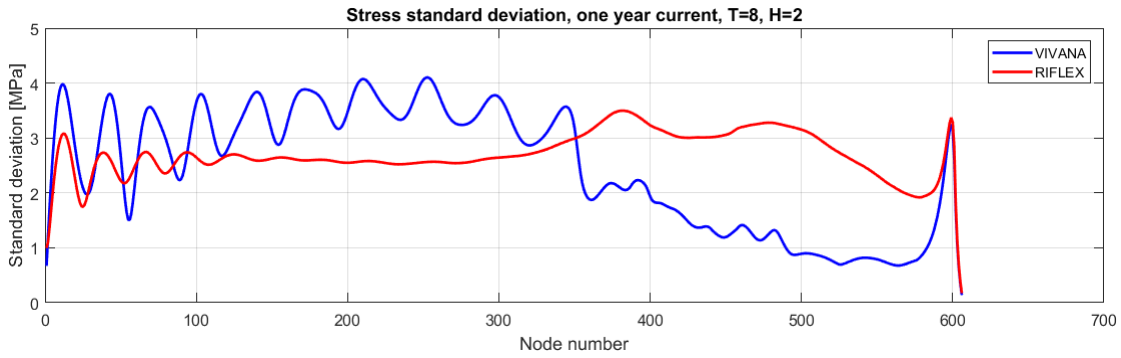

Figure 8.16: Stress standard deviation for a typical one year extreme current and waves with Hs=2m and T=8s.

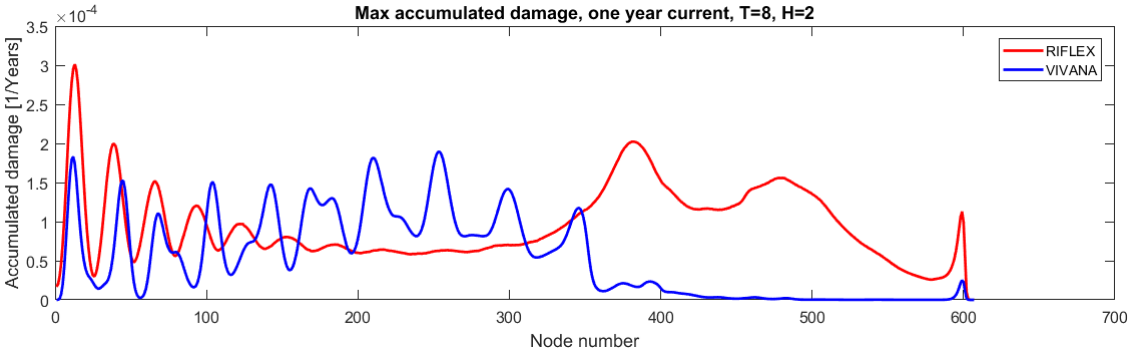

Figure 8.17: Maximum accumulated damage for a typical one year extreme current and waves with Hs=2m and T=8s.

Scenario 2

The stress standard deviation for scenario two is presented in Figure 8.18. The peak from the current practice at the upper half have smoothed even more out for this scenario than the one before. The peak from the wave contribution is included at the top of the riser. The stress standard deviation from RIFLEX lies above the one for the current practice. The same observations as for the stress standard deviation is found in Figure 8.19 for the maximum accumulated damage.

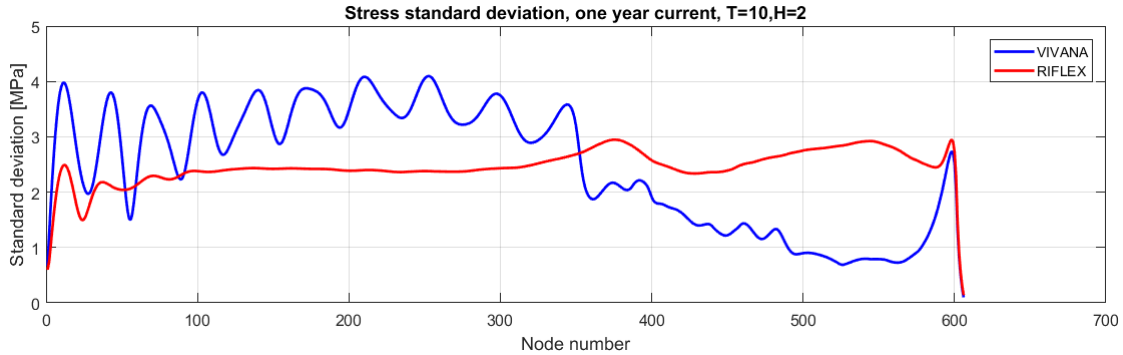

Figure 8.18: Stress standard deviation for a typical one year extreme current and waves with Hs=2m and T=10s.

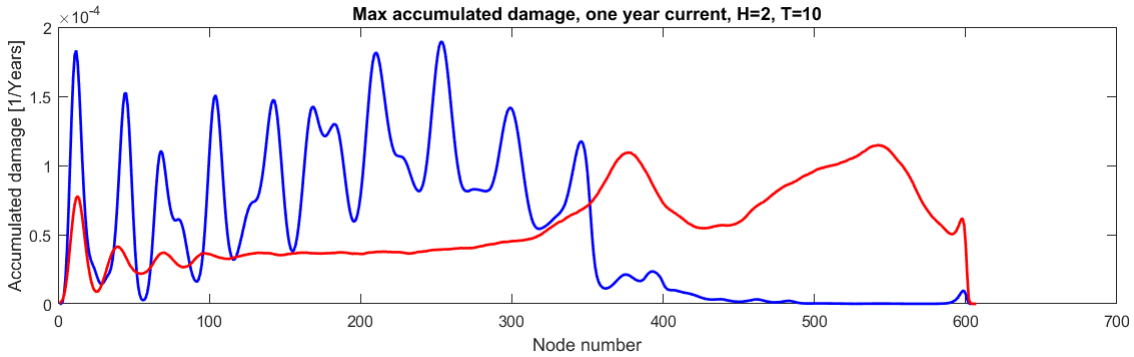

Figure 8.19: Maximum accumulated damage for a typical one year extreme current and waves with Hs=2m and T=10s.

Scenario 3

For the third scenario is the wave height higher than the two before. This is seen from the peak in the stress standard deviation in Figure 8.20, which is higher at the top of the riser than the once before. In the maximum accumulated damage in Figure 8.21 is the damage higher for RIFLEX in the top of the riser, while the damage at the bottom of the riser is higher for the current practice than for RIFLEX.

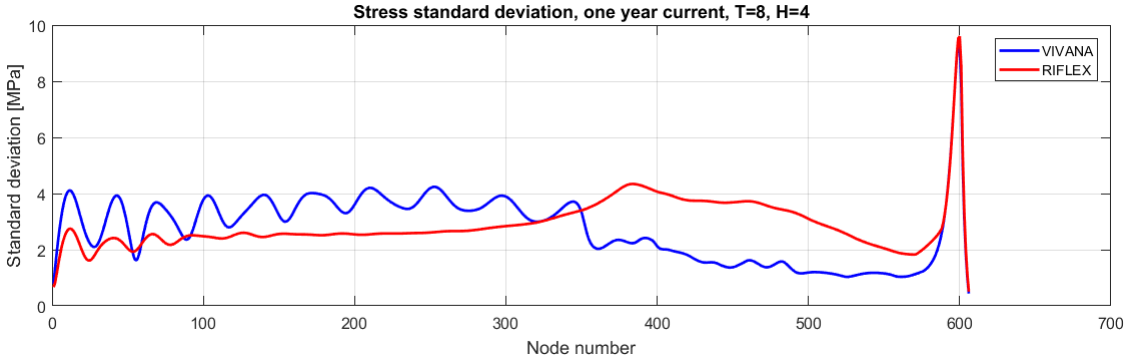

Figure 8.20: Stress standard deviation for a typical one year extreme current and waves with Hs=4 and T=8.

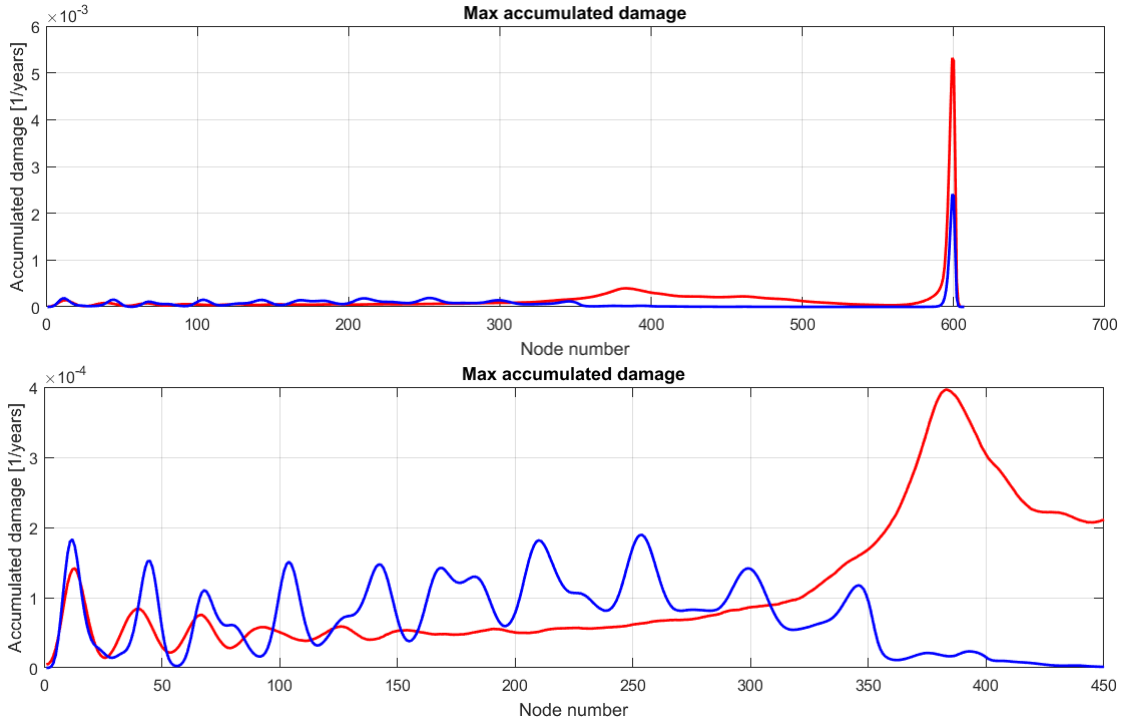

Figure 8.21: Maximum accumulated damage for a typical one year extreme current and waves with Hs=4 and T=8s.

Scenario 4

The stress standard deviation in Figure 8.22 has the same shape as the stress standard deviation in scenario three, but fairly higher values due to increase of the wave height from 2 meters to 4 meters. The maximum accumulated damage in Figure 8.23 shows the same similarities.

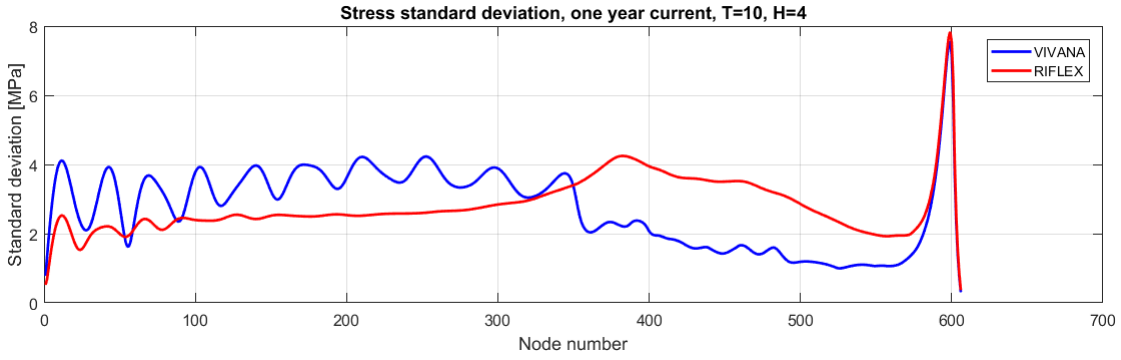

Figure 8.22: Stress standard deviation for a typical one year extreme current and waves with Hs=4m and T=10s.

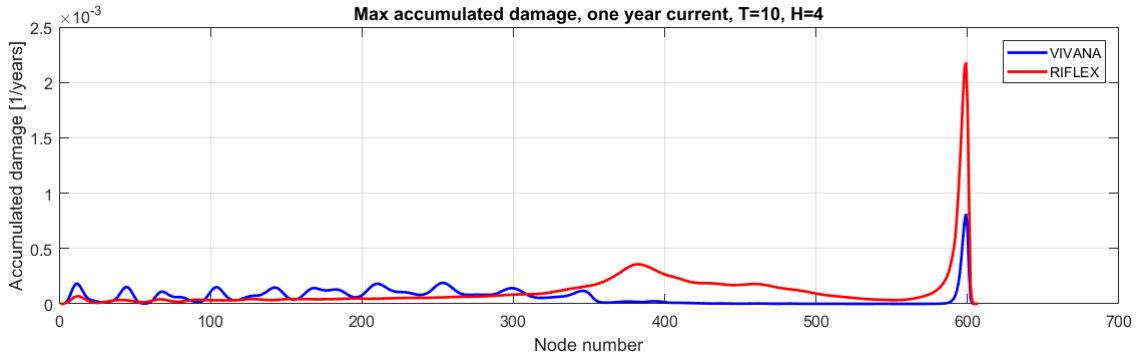

Figure 8.23: Maximum accumulated damage for a typical one year extreme current and waves with Hs=4m and T=10s.

Evaluating of scenarios

The huge differences between the current practice and the new time domain model in RIFLEX occurs before waves are acting, and are due to the calculation of excitation zones in VIVANA. If another approach than simultaneously active frequencies were used the result form VIVANA could be different. This deviation for the two model follows in the different scenarios of wave heights and wave periods.

The current in this case compared to the one in first case is much greater. The new time domain analysis in RIFLEX have a peak at the upper part of the riser which decreases when waves are acting. This is due to the velocity of the water. When current is the only external force that is acting are the water particles velocity only due to current velocity. In contrast to this is the water particle velocity affected by both the waves and the current for all the scenarios presented. Due to this is the peak in the upper half of the riser in the time domain analysis reduced when waves are applied.

As for case one is the maximum accumulated damage different for the current practice and the new time domain analysis even when the stress standard deviation is equal. As mention earlier is this due to the super-positioning of the current practice, where the stress in the power of four gives a huge different for the two methods.

8.3.3 Case 3

The maximum accumulated damage is presented for the current practice and the new time domain model, with and without RAO. This is done to see the impact that the RAO have on the different methods.

Scenario 1

The accumulated damage for the first scenario is presented in Figure 8.24. The maximum accumulated damage from RIFLEX has decreased in the bottom of the riser and increased in the top. For the current practice has the maximum accumulated damage increased in the top of the riser, and no bug changes in the bottom of the riser. The new time domain model is more affected by the RAOs in the bottom of the riser than current practice.

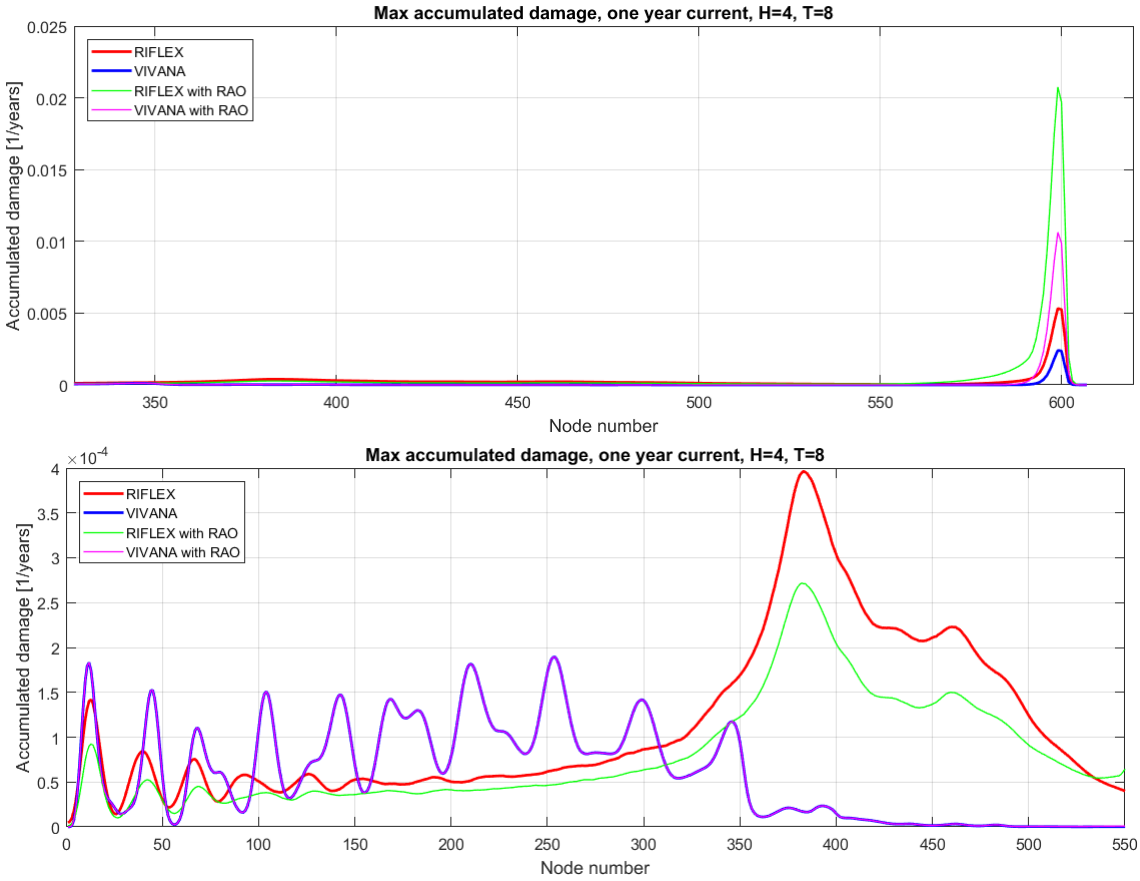

Figure 8.24: Maximum accumulated damage for a typical one year extreme current and waves with Hs=4 and T=8s.

Scenario 2

The maximum accumulated damage for this scenario is presented in Figure 8.25. The maximum accumulated damage from RIFLEX with RAO is slightly below the one without RAO, this regards the whole riser. The hugest difference between the one with RAO and the one without is at the top of the riser. There is no big changes for the current practice in the bottom of the riser with respect to RAO. At the top of the riser is the maximum accumulated damage without RAO higher than the one with

RAO.

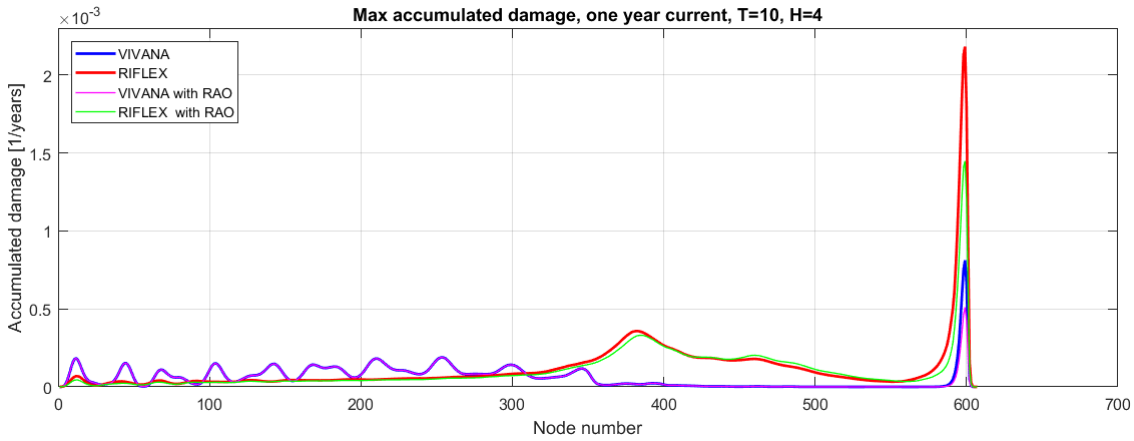

Figure 8.25: Maximum accumulated damage for a typical one year extreme current and waves with Hs=4m and T=10s.

Evaluation of scenarios

When RAO is included in the analysis no big differences is seen. The largest distinction when RAO is applied is at the top of the riser, close to the semisumbmersible. For one of the scenarios is the maximum accumulated damage higher than the one without RAO, while for the other one is the maximum damage lower. The transfer functions in the RAO file is dependent on the period of the waves, which is seen since the maximum accumulated damage get a positive and a negative contribution when wave period is the only parameter that is changed. It is also seen that the new time domain model is more affected by the RAOs than the current practice, especially at the bottom of the riser.

Chapter 9

Conclusion and recommendations for further work

9.1 Conclusion

In this thesis the new time domain model developed by PhD. Mats J. Thorsen compared with the current practice with respect to fatigue of a drilling riser. Both methods have investigated the same drilling riser and are exposed to the same environmental loads.

The two methods shown good agreement for the stress standard deviation for all scenarios in the first case investigated. The maximum accumulated damage on the other hand showed good agreement for the scenario without waves but some deviations when waves were applied. This is due to the calculations of fatigue by superposition for the current method that underestimates the damage.

The results for the second case showed huge differences, which have to do with the approach VIVANA uses to calculate excitation zones. When waves were applied, there was a distinct stress increase in the top of the riser. This was the case for both of the methods.

In the third case was RAOs included in the analysis. The new time domain model was more affected by the RAOs than the current practice. Both methods showed and changes in the top of the riser, increase or decrease of the maximum accumulated damage dependent on the wave parameters.

The most important difference between the methods is the way fatigue damage is calculated. The current practice underestimates the maximum accumulated damage by use of superposition. Based on this the new time domain model is calculating a more accurate fatigue damage than the current practice.

9.2 Further work

In this thesis is two current profiles investigated for the compliance of the current practice and the new time domain model. More case studies can be performed with other current profiles and different heading of the waves. In addition to this other pipelines with different structural properties can be investigated. Only The CF direction have been investigated, for further studies IL direction could also be studied with respect to compliance of the methods.

The two models showed huge differences in the results for one of the current profiles. To investigate this more, other options for frequency response in VIVANA could be examined. It would also be beneficial to compare both of the methods with experimental methods, at least for the current where it was huge deviations between the methods. In addition it could be interesting to compare the methods to data from full scale experiments to see how the models respond compared to realistic data.

Bibliography

[1] Robert D. Blevins. *Flow-induced vibration.* Van Nostrand Reinhold, New York, 2nd ed. edition, 1990.

[2] Carl M. Larsen. Vortex induced vibrations; a short and incomplete introduction to fundamental concepts. 2011.

[3] DNV. *DNV-RP-C203 Fatigue Design of Offshore Steel Structures.* 2011.

[4] Christian Boller and Matthias Buderath. Fatigue in aerostructures: Where structural health monitoring can contribute to a complex subject. *Philosophical Transactions: Mathematical, Physical and Engineering Sciences*, 365(1851):561–587, 2007.

[5] Mats Jørgen Thorsen, teknikk Norges teknisk-naturvitenskapelige universitet Institutt for marin, and universitet Norges teknisk naturvitenskapelige. *Time domain analysis of vortex-induced vibrations.* Thesis, 2016.

[6] Odd M. Faltinsen. *Sea loads on ships and offshore structures.* Cambridge ocean technology series. Cambridge University Press, Cambridge, 1990.

[7] Marilene Greco. Tmr 4215: Sea loads, lecture notes. 2012.

[8] Kyrre Vikestad. *Multi-frequency response of a cylinder subjected to vortex shedding and support motions.* Thesis, 1998.

[9] R. D. Gabbai and H. Benaroya. An overview of modeling and experiments of vortex-induced vibration of circular cylinders. *Journal of Sound and Vibration*, 282(3):575–616, 2005.

[10] Computational fluid dynamics (cfd). `http://whatis.techtarget.com/definition/computational-fluid-dynamics-CFD`.

[11] O. K. Kinaci, S. Lakka, H. Sun, and M. M. Bernitsas. Effect of tip-flow on vortex induced virbation of circular cylinders for re$< 1.2 * 10^5$. 2015.

[12] Mohd Asamudin A. Rahman, Jeremy Leggoe, Krish Thiagarajan, Mohd Hairil Mohd, and Jeom Kee Paik. Numerical simulations of vortex-induced vibrations on vertical cylindrical structure with different aspect ratios. *Ships and Offshore Structures*, pages 1–19, 2015.

[13] Carl M. Larsen and Karl H. Halse. Comparison of models for vortex induced vibrations of slender marine structures. *Marine Structures*, 10(6):413–441, 1997.

[14] T. Sarpkaya. Fluid forces on oscillating cylinders. *Journal of the Waterway, Port, Coastal and Ocean Division*, 1978.

[15] MIT AMOG Consulting. User guide got shear7 version 4.9b. 2016.

[16] R. Grant, R Litton, L. Finn, J. Maher, and K. Lambrakos. Highly compliant rigid riser: Field test benchmarking a time domain viv algorithm. *Proceedings of the Offshore Technology Conference, Houston*, 2000.

[17] Peter Ma, Wei Qiu, and Don Spencer. Numerical vortex-induced vibration prediction of marine risers in time-domain based on a forcing algorithm.(author abstract). *Journal of Offshore Mechanics and Arctic Engineering*, 136(3):31703, 2014.

[18] Jørgen Amdahl, Leif Lundby, and marin Samarbeidsforum. *Havromsteknologi : et hav av muligheter*. NTNU, Samarbeidsforum marin, Trondheim, 2013.

[19] Marit Irene Kvittem and teknikk Norges teknisk-naturvitenskapelige universitet Institutt for marin. *Modelling and response analysis for fatigue design of a semi-submersible wind turbine*. Thesis, 2014.

[20] Fridtjov Irgens. *Statikk og fasthetslære : B. 1 : Statikk*, volume B. 1. Tapir, Trondheim, 3. utg. edition, 1985.

[21] R. I. Stephens and H. O. Fuchs. *Metal fatigue in engineering*. J. Wiley, New York, 2nd ed. edition, 2001.

[22] DNV. *DNV-RP-F204 Riser Fatigue*. 2010.

[23] International Organization for Standardization. *ISO 13623 - Petroleum and natural gas industries - Pipeline transportation systems*. 2000.

[24] DNV. *DNV-RP-C205 Environmental Conditions and Environmental Loads*. 2010.

[25] MARINTEK. Riflex theory manual v4.2v0. 2014.

[26] MARINTEK. Riflex user's manual v4.2rev0. 2014.

[27] Carl M. Larsen, Halvor Lie, Elizabeth Passano, Rune Yttervik, Jie Wu, and Gro Baarholm. Vivana - theory manual version 3.7. 2009.

[28] MARINTEK. Vivana 4.8.2 user guide. 2016.

[29] Svein Sævik. Simla - theory manual revised as of 2008-06-06. 2008.

[30] Torgeir Moan. *Finite element modelling and analysis of marine structures*, volume UK-03-98 of *Kompendium (Norges teknisk-naturvitenskapelige universitet. Institutt for marin teknikk)*. Department of Marine Technology, Norwegian University of Science and Technology, Trondheim, 2003.

[31] Ivar Langen and Ragnar Sigbjörnsson. *Dynamisk analyse av konstruksjoner*. Utdrag fra Dynamisk analyse av konstruksjoner. s.n., S.l., 1999.

[32] WAFO-group. *WAFO - A Matlab Toolbox for Analysis of Random Waves and Loads - A Tutorial*. Math. Stat., Center for Math. Sci., Lund Univ., Lund, Sweden, 2000.

Appendix A

Input Files

A.1 INPMOD

```
'************************************************************************
 INPMOD IDENTIFICATION TEXT 4.6.1
'************************************************************************



'------------------------------------------------------------------------
 UNIT NAMES SPECIFICATION
'------------------------------------------------------------------------
'ut ul um uf grav gcons
 s  m  Mg kN /   1.000000000e+00
'************************************************************************
 NEW SINGLE RISER
'************************************************************************
'atyps idris
 AR   ARSYS
'************************************************************************
 ARBITRARY SYSTEM AR
'************************************************************************
'nsnod nlin nsnfix nves nricon nspr nakc
 2    1   2     0   0     1   0
'ibtang zbot           ibot3d
 1     -1.2000000000e+03 0
'stfbot        stfaxi        stflat        friaxi        frilat        dambot        damaxi        damlat
 1.0000000e+03 1.0000000e+01 5.0000000e+01 5.0000000e-01 8.0000000e-01 0.0000000e+00 0.0000000e+00 0.0000000e+00
'B 6.5: LINE TOPOLOGY DEFINITION
'lineid lintyp-id snod1-id snod2-id
 line1  ltyp1    node1    node2
'FIXED NODES
'snod-id ipos ix iy iz irx iry irz chcoo  chupro
 node1  0   1  1  1  0   0   1   GLOBAL NO
'x0           y0           z0           x1           y1           z1           rot          dir
 0.0000000e+00 0.0000000e+00 -1.20000000e+03 0.0000000e+00 0.0000000e+00 -1.20000000e+03 0.0000000e+00 0.0000000e+00
'snod-id ipos ix iy iz irx iry irz chcoo  chupro
 node2  0   1  1  0  0   0   1   GLOBAL NO
'x0           y0           z0           x1           y1           z1           rot          dir
 0.0000000e+00 0.0000000e+00 1.2000000e+01 0.0000000e+00 0.0000000e+00 1.20000000e+01 0.0000000e+00 0.0000000e+00
'FREE NODES
'line-id iseg inod ildof stipar         damp         a2
 line1  1   607 3    -3.000000000e+00 0.00000000e+00 0.000000000e+00
'PON(i) DISPL(i)
 -1.001000000e+03 -1.000000000e+00  &
 -1.000000000e+03 0.000000000e+00  &
 -9.990000000e+02 1.000000000e+00
'B.10 Line and segment specification
```

```
'*************************************************************************
 NEW LINE DATA
'*************************************************************************
'lintyp-id nseg ncmpty2 flutyp iaddtwi iaddbend
 ltyp1    1   0      0    0      0
'crstyp ncmpty1 exwtyp nelseg slgth          nstrps nstrpd slgth0         isoity
 cs1_1 0      0     606   1.212000000000e+03 /     /     5.000000000e+02 0
'*************************************************************************
 NEW COMPONENT CRS1
'*************************************************************************
'cmptyp-id temp          alpha         beta
 cs1_1    2.000000000e+01 0.000000000e+00 0.000000000e+00
'ams           ae            ai            rgyr          ast wst dst thst rextcnt rintcnt
 1.400000000e-01 7.070000000e-02 6.160000000e-02 0.000000000e+00 0  0  0  0   0     0
'iea iej igt ipress imf harpar
 1  1  1  0     0  0.000000000e+00
'ea
 1.910000000e+06
'ei           gas
 2.010000000e+04 0.000000000e+00
'gtminus
 1.340000000e+04
'chload
 HYDR
'chtype
 TVIV
'cqx           cqy           cax           cay           clx           cly           icode d   scfk          Cv   FNUL FMIN  FMAX NMEM
 0.0000000e+00 1.300000e+00 0.0000000e+00 1.0000000e+00 0.0000000e+00 0.0000000e+00 2     0.3 1.0000000e+00 1.0 0.19 0.125 0.3  500
'tb            ycurmx
 1.000000000e-03 1.000000000e+00
'*************************************************************************
 ENVIRONMENT IDENTIFICATION
'*************************************************************************

'idenv
 ENV
'-------------------------------------------------------------------------
 WATERDEPTH AND WAVETYPE
'-------------------------------------------------------------------------
'wdepth         noirw norw ncusta nwista
 1.200000000e+03 0    1    1     0
'-------------------------------------------------------------------------
 ENVIRONMENT CONSTANTS
'-------------------------------------------------------------------------
'airden         watden         wakivi         airkivi
 1.300000000e-03 1.025000000e+00 1.000000000e-06 1.880000000e-06
'-------------------------------------------------------------------------
 REGULAR WAVE DATA
'-------------------------------------------------------------------------
'inrwc amplit  period       wavdir
 1    4      10                                    270.000000000e+00
'-------------------------------------------------------------------------
 NEW CURRENT STATE
'-------------------------------------------------------------------------
'icusta nculev l_ext
 1     12    0
'curlev         curdir         curvel
 0.000000000e+00 0.000000000e+00 0.980000000e+00
 -2.000000000e+01 0.000000000e+00 0.980000000e+00
 -5.000000000e+01 0.000000000e+00 0.890000000e+00
 -1.000000000e+02 0.000000000e+00 8.20000000e-01
 -2.000000000e+02 0.000000000e+00 7.500000000e-01
 -3.000000000e+02 0.000000000e+00 6.300000000e-01
 -4.000000000e+02 0.000000000e+00 7.200000000e-01
 -5.000000000e+02 0.000000000e+00 4.600000000e-01
 -6.000000000e+02 0.000000000e+00 4.600000000e-01
 -8.000000000e+02 0.000000000e+00 4.500000000e-01
 -1.000000000e+03 0.000000000e+00 4.400000000e-01
 -1.200000000e+03 0.000000000e+00 4.100000000e-01
'*************************************************************************
 END
'*************************************************************************
```

A.2 STAMOD

```
'A1       STAMOD IDENTIFICATION TEXT
'************************************************************************
 STAMOD CONTROL INFORMATION 4.6.1
'************************************************************************



'A1.3   OPTION AND PRINT SWITCHES
'irunco idris ianal iprdat iprcat iprfem ipform iprnor ifilm ifilco
 1     ARSYS 1    2     1     1     1     1     2    0
'------------------------------------------------------------------------
 RUN IDENTIFICATION
'------------------------------------------------------------------------
'idres
 SIMA
'------------------------------------------------------------------------
 ENVIRONMENT REFERENCE IDENTIFIER
'------------------------------------------------------------------------
'idenv
 ENV
'------------------------------------------------------------------------
 STORE VISUALISATION RESPONSES
'------------------------------------------------------------------------
'option chresp chilin
 STORE  ALL    ALL
'************************************************************************
 STATIC CONDITION INPUT
'************************************************************************
'lcomp icurin curfac         iwindin
 0    1     1.000000000e+00 0
'lcons isolvr
 0    2
'************************************************************************
 COMPUTATIONAL PROCEDURE
'************************************************************************
'ameth
 FEM
'------------------------------------------------------------------------
 FEM ANALYSIS PARAMETERS
'------------------------------------------------------------------------
'.....................................................................
 LOAD GROUP DATA
'.....................................................................
'nstep maxit racu
 10    10    1.000000000e-06
'lotype ispec
 SPRI   0
```

```
'.....................................................................
 LOAD GROUP DATA
'.....................................................................
'nstep maxit racu
 10   10   1.000000000e-06
'lotype ispec
 VOLU  0
'.....................................................................
 LOAD GROUP DATA
'.....................................................................
'nstep maxit racu
 100   100   1.000000000e-06
'lotype ispec
 CURR  0
'**********************************************************************
 END
'**********************************************************************
```

A.3 DYNMOD

```
'A1       DYNMOD CONTROL INFORMATION
'************************************************************************
 DYNMOD CONTROL INFORMATION 4.6.1
'************************************************************************



'irunco ianal   idris idenv idstat idirr idres
 ANAL   REGULAR ARSYS ENV   SIMA   XX    SIMA
'************************************************************************
'
'         DATA GROUP C, REGULAR WAVE, TIME DOMAIN ANALYSIS
'
'************************************************************************
 REGULAR WAVE ANALYSIS
'************************************************************************
'nper nstppr irwcn imotd
 360    800    1    0
'************************************************************************
 REGULAR WAVE LOADING
'************************************************************************
'iwtyp isurf iuppos
 1    1    2
'************************************************************************
'
'         DATA GROUP E
' Time domain procedure and file storage parameters
'
'************************************************************************
 TIME DOMAIN PROCEDURE
'************************************************************************
'itdmet inewil
 2     1
'E1.3   TIME INTEGRATION
'betin          gamma          theta          a1             a2             a1t            a1to           a1b            a2t            a2t0           a2b
 4.000000000e+00 5.000000000e-01 1.000000000e+00 0.000000000e+00 7.000000000e-03 0.000000000e+00
0.000000000e+00 0.000000000e+00 0.000000000e+00 0.000000000e+00 0.000000000e+00 0.000000000e+00
'E1.4    NONLINEAR FORCE MODEL
'indint indhyd maxhit epshyd         tramp          indrel iconre istepr ldamp
 1     1     5     1.000000000e-02 1.000000000e+01 0     0     0     0
'------------------------------------------------------------------------
 NONLINEAR INTEGRATION PROCEDURE
'------------------------------------------------------------------------
'itfreq isolit maxit daccu          icocod ivarst itstat
 1     1     10    1.000000000e-05 1     0     1
```

```
'-------------------------------------------------------------------
 DISPLACEMENT RESPONSE STORAGE
'-------------------------------------------------------------------
'idisp nodisp idisfm
 5    1     -1
'line-id iseg inod
 line1   1    ALL
'-------------------------------------------------------------------
 FORCE RESPONSE STORAGE
'-------------------------------------------------------------------
'ifor nofor iforfm ieltfm
 5   1    -1    0
'line-id iseg iel
 line1   1    ALL
'-------------------------------------------------------------------
 ENVELOPE CURVE SPECIFICATION
'-------------------------------------------------------------------
'ienvd ienvf ienvc tenvs          tenve          nprend nprenf nprenc ifilmp
 0    0    0    0.000000000e+00 1.000000000e+07 0     0     0     2
'
STORE VISUALISATION RESPONSES
'
'TCONDS TCONDE DELT CHFORM
 0       50   0.0625  VIS
'************************************************************************
 END
'************************************************************************
```

Appendix B

MATLAB scripts and Input Files

All the MATLAB scripts and Input Files have been uploaded as an electronical appendix in a .zip file which contains the following:

Folder	**Content**
Case_studies	All input files for the different cases and scenarios. See README.txt in folder on how to run the analyses.
MATLAB	All MATLAB files for calculating the fatigue damage as well as the stress standard deviation are included in this folder. Se the README.txt file in the folder for more information.
Poster	Contribution to the poster contest held at Marinteknisk Senter.